https://doi.org/10.57634/RCR5074

Selective recovery and re-utilization of lithium: prospects for the use of membrane methods

Dmitrii Yu. Butylskii,[a] Lasâad Dammak,[b] Christian Larchet,[b] Natalia D. Pismenskaya,[a] Victor V. Nikonenko [a]*

[a] *Kuban State University, ul. Stavropolskaya 149, 350040 Krasnodar, Russian Federation*
[b] *Université Paris-Est Créteil, CNRS, ICMPE, UMR 7182, 2 rue Henri Dunant, Thiais, 94320 France*

In recent years, due to the sharp increase in lithium demand, the interest in the problem of lithium recovery/extraction has increased dramatically: according to the Scopus database, ~3000 scientific publications on this issue appeared in 2021. The efforts of many specialists are directed towards the development of new, more economical and environmentally safe membrane technologies for lithium recovery to replace the existing reagent-based methods. This review integrates up-to-date data about the traditional and prospective methods for lithium recovery from natural solutions and leachates resulting from the disposal of spent batteries. The attention is focused on membrane methods. Known approaches are classified and analyzed, experimental and theoretical aspects of membrane-based ion separation are described; separation mechanisms and mathematical models are discussed. The review addresses pressure-driven and electromembrane processes, relatively well-developed at a laboratory level, which are used to extract lithium and other singly charged ions from mixed solutions containing large amounts of magnesium and calcium. The results of application of commercial and laboratory-made membranes are compared. Novel and emerging approaches suitable for effective separation of lithium ions from a mixture of singly charged cations, including hybrid electrobaromembrane methods, are considered.
The bibliography includes 295 references.

Contents

1. Introduction

Lithium element has been known for more than 200 years; however, its wide application started not long ago. In 1976, M.Stanley Whittingham invented and patented the first viable lithium-based battery; somewhat later, J.B.Goodenough suggested using cobalt-based materials (lithium cobalt oxide) in these batteries. More recently, a research team headed by A.Yoshino developed a lithium-ion battery (LIB), which was further commercialized by Sony corporation.[†]

[†] For the development of lithium-ion batteries, M.S.Whittingham, J.B.Goodenough and A.Yoshino were awarded the Nobel Prize in Chemistry (see, for example, https://nplus1.ru/news/2019/10/09/nobel-chemistry-2019).

Received 25 November 2022

Nowadays, lithium is widely used in various fields of modern industry. This is related, first of all, to the rapid development of the production of rechargeable LIBs,[1–3] which are used for energy concentration and storage. The role of these devices is especially significant for the development of the renewable energy infrastructure. This is manifested as gradual transformation of the existing energy consumption structure from natural energy sources to renewable ones. According to prediction of many researchers, the proportion of energy derived from renewable sources would increase in the future, which is expected to reduce the CO_2 emission to the atmosphere.[4–7]

Other applications of lithium, such as food and pharmaceutical industries, aviation and aerospace sectors, electrical engineering, nuclear power engineering and manufacture of ceramics, glass, lubricants, synthetic rubber, *etc.*, are less abundant, but no less significant.[8] Specialists agree that lithium is one of the critically important chemical elements for the development of the world economy and that efficient lithium production is a priority for the strategic development of many countries.[2,8,9]

There are three main sources of lithium:

— hard rock minerals;

— highly concentrated natural solutions of lithium salts (mine waters, formation waters, brines, *etc.*);

— spent LIBs.

Historically, traditional sources of lithium are minerals. Lithium is mainly extracted from spodumene and lepidolite, which are found in pegmatite rock formations. However, pegmatite is quite difficult to process due to its hardness and problematic access to the belt rocks in which it is commonly found. Currently, Australia is the world largest producer of lithium from minerals, mainly from spodumene (Fig. 1).[10] The lithium content in Australian spodumene is, most often, 1 to 3% in terms of Li_2O.[11–13] In 2021, the world reserves of lithium present in minerals were estimated at ~22 million tons. However, this value is revised every year and naturally increases as new data gained from continuing exploration are taken into account.

In recent years there has been a tendency to obtain lithium from natural aqueous solutions (brines, formation and mine waters, *etc.*). According to various national geological surveys, lithium resource in natural waters around the world is ~89 million tons.[15,17,18] These solutions may be directly exposed to the surface or hidden deep underground in salt lakes found in very arid regions. Most of the global lithium resources existing in natural waters are located in the so-called lithium triangle consisting of Bolivia, Argentina and Chile.[3,19]

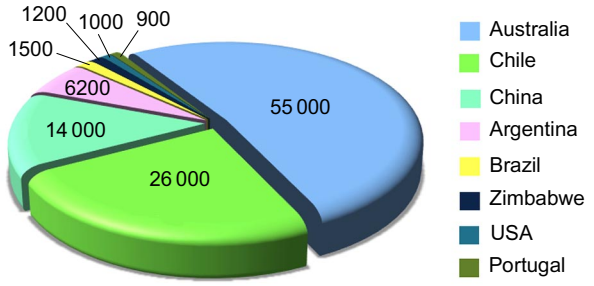

Figure 1. Contributions of countries to the world mine production of lithium in 2021 (tons per year). The Figure was created by the authors using published data.[14–16]

Thus, the total world reserves of lithium are currently estimated to be ~110 million tons. Considering the current rate of its production amounting to 105 thousand tons per year, these reserves will last for about the next 1000 years. Due to the above-noted lithium demand in various industries, lithium recovery techniques have attracted attention of a lot of researchers.

The problem of lithium production is a hot topic in the scientific literature. In recent years, more than a dozen reviews have appeared. Along with traditional reagent-based methods for the recovery/extraction of lithium, these publications address the prospects for using membrane methods to solve this problem.[11,20–28] Researchers paid attention to both pressure-driven (baromembrane)[24–26] and electromembrane methods[20,21,23] for selective extraction of lithium from brines and extracts containing multiply charged (mainly, doubly charged Ca^{2+}, Mg^{2+}, Ni^{2+}, Mn^{2+} and Co^{2+}) ions.

In this review, we have tried to cover up-to-date information on both traditional and prospective methods for the production/extraction of lithium. The main emphasis is placed on the description of membrane methods for lithium recovery from aqueous solutions containing simultaneously multiply charged and singly charged (mainly Na^+ and K^+) ions. The literature and our own estimates of the efficiency of membrane processes in comparison with reagent-based methods are given. Apart from the commonly used characteristics (such as specific energy consumption and the highest degree of purity of the lithium product[20,22,27,28]), we estimated the separation rate (transmembrane fluxes for the extracted lithium and competing ions). In addition to the baromembrane and electromembrane methods, the prospects for hybrid electrobaromembrane processes using two driving forces simultaneously are discussed for the first time; the efficiency of such processes for the separation of monovalent cations is shown. Along with the achievements of recent experimental studies, this review also presents the physicochemical fundamentals necessary for the understanding and mathematical modelling of the phenomena that determine the ion separation in baro- and electromembrane processes.

2. Traditional reagent-based methods for lithium recovery

2.1. Recovery from minerals

Lithium does not occur in nature in the free state, but its compounds are found in many igneous rocks and natural

D.Yu.Butylskii. PhD in Chemistry, Senior Researcher, Associate Professor at the Department of Physical Chemistry, KubSU.
E-mail: d_butylskii@bk.ru
L.Dammak. Professor at the Université Paris-Est Créteil.
E-mail: dammak@u-pec.fr
Ch.Larchet. Professor at the same University.
E-mail: larchet@u-pec.fr
N.D.Pismenskaya. Doctor of Chemical Sciences, Professor at the Department of Physical Chemistry, KubSU.
E-mail: n_pismen@mail.ru
V.V.Nikonenko. Doctor of Chemical Sciences, Professor at the same Department.
E-mail: v_nikonenko@mail.ru
Current research interests of the authors: ion-exchange materials and related processes, concentration, and desalination of aqueous solutions, selective recovery of valuable components

Translation: Z.P.Svitanko

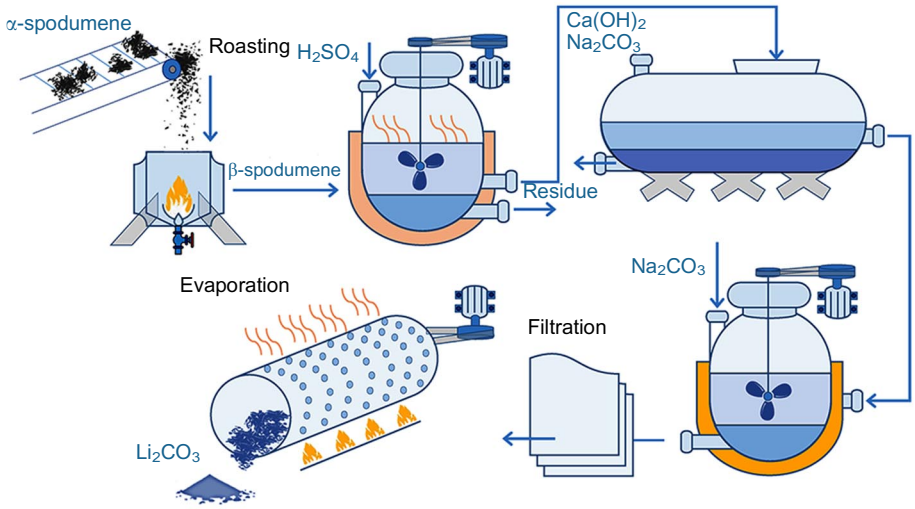

Figure 2. Flow diagram of the process of Li^+ extraction from spodumene concentrate. For the sequence and description of stages, see the text. The Figure was created by the authors using published data.[12, 13, 31]

waters, into which they are extracted as a result of geological processes.[29] Out of more than 20 known minerals containing lithium, only four (spodumene, lepidolite, petalite and amblygonite) are of industrial interest because of the relatively high lithium content in these minerals.[3] The pegmatite, cookeite, taeniolite and lithiophorite minerals are considered to be unprofitable sources of lithium. Spodumene ($LiAlSi_2O_6$) is used most often to produce lithium carbonate.[30, 31] The traditional methods for the production of lithium carbonate from spodumene can be described by the simplified flow diagram shown in Fig. 2.

The sulfuric acid process is used most often for lithium extraction from spodumene.[12] Mined natural spodumene (α-spodumene), which has a monoclinic structure, is subjected to high-temperature pretreament (roasting) at 1100 °C to obtain more chemically reactive β-spodumene (tetragonal structure).[13] Then β-spodumene is cooled down, ground, and heated again (200–250 °C) in a kiln with an excess of concentrated sulfuric acid. The purpose of the sulfuric acid process is to recover lithium from the mixture in the form of water-soluble lithium sulfate. This is done using a 30–40% excess of the acid. Apart from the main product, the reaction gives a large amount of waste as an insoluble ore residue. The residue is separated and the remaining solution is filtered. Then, to remove magnesium from the lithium concentrate, lime (calcium hydroxide) is used, and sodium carbonate is used to remove residual calcium. The resulting solution is concentrated by evaporation. The degree of lithium extraction as Li_2CO_3 can be increased by adding an excess of sodium carbonate. A high degree of purification is achieved by conducting additional chemical or physical treatment.[32, 33]

The traditional commercial production of lithium from natural minerals such as spodumene can provide a high degree of extraction (>90%); however, this process is rather resource-, energy- and labour-intensive and generates huge quantities of waste.[34] In addition, the purity of lithium carbonate obtained in this process corresponds to technical grade (~95%). Battery grade lithium carbonate should be at least 99.5% pure, which is achieved through additional purification.[35, 36]

Data on the production costs for this process are difficult to find in the literature; they are usually published as parts of NI 43-101 or JORC reports.[37–40] According to published data,[15, 37, 40] the cost of production of lithium carbonate from rock minerals by the above-described process is economically viable.

2.2. Extraction from natural brines

The production of lithium-containing brines is associated with lower exploration, capital and operation costs[41] and also resource costs compared to mining of solid minerals. Among other causes, the last-mentioned circumstance is due to the fact that, after being extracted from a natural source, a lithium-containing brine is concentrated, most often, through evaporation under natural conditions in evaporation ponds under the action solar light (Fig. 3). Simultaneously, some mineral components (primarily Ca^{2+} and Mg^{2+}) are precipitated by adding an excess of HCl for the subsequent crystallization of $CaCl_2$. In the next stage, an excess of NaOH is added to separate solid precipitates, and then sodium carbonate is added to remove residual calcium. A cleaner concentrate is obtained when these processes are alternated with the separation of solid and liquid phases. Then an excess of sodium carbonate is added with the appropriate pH adjustment to recover lithium as Li_2CO_3.[42] The solubility of lithium carbonate is 1 g per 100 g of water at 50 °C, while lowering the temperature leads to increasing solubility. At the final stages, the Li_2CO_3 precipitate is filtered to remove excess water and then dried. According to King and Dworzanowski,[42] the overall lithium recovery is 51%, and the purity of the resulting lithium carbonate corresponds to battery grade (⩾ 99.5%). Owing to availability of raw materials in the form of brines, the production of battery grade lithium carbonate usually shows a significantly positive net present value.[42, 44]

However, the production of lithium from brines requires a lot of space to place evaporation ponds (for example, ~450 hectares are needed to produce 20 thousand tons of lithium carbonate per year[42]). Furthermore, in the first stage of brine processing using evaporation ponds, the desired concentration is attained only after 12–24 months;[43] hence, these production facilities are constructed only in the arid Lithium Triangle region of Latin America.

2.3. Extraction from spent batteries

The recovery of lithium from spent lithium-ion batteries (LIBs) has the following advantages: high concentration of lithium and other valuable metals (cobalt, nickel, manga-

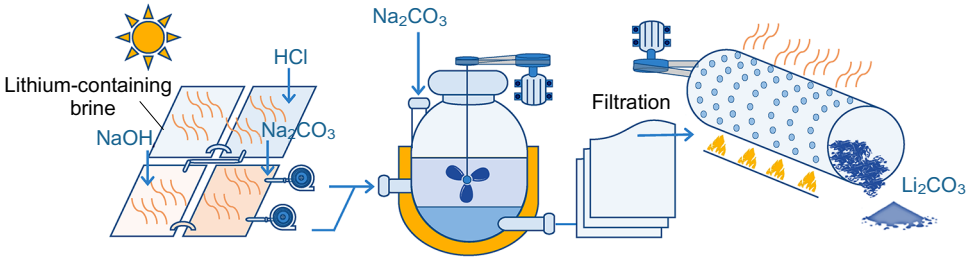

Figure 3. Flow diagram of the process of Li^+ extraction from natural brines. For the sequence and description of stages, see the text. The Figure was created by the authors using published data.[42,43]

nese, *etc.*); relatively low concentrations of ions that are of little value (such as Ca^{2+} and Mg^{2+} present in minerals and brines); reduction of environmental burden due to the neutralization of hazardous waste; *etc.*[45] Meanwhile, recycling of spent batteries is a fairly complicated task. This is mainly due to the necessity to classify different types of batteries, complexity of their disassembly and high reactivity of materials present in spent LIBs, which can ignite and explode on contact with air.[46] In addition, it is worth noting that according to the data of the United State Geological Survey,[15] at least about a third of global lithium production in 2021 was used to make products other than batteries, such as ceramics and glass, lubricating greases, casting powders, *etc.* This means that this part of lithium cannot be recycled, as this process is not economically justified. Furthermore, lithium recycled from LIBs is rarely used again in batteries;[47,48] most often, it is used in lubricants and other products in which high purity is not required.

In most countries, only a minor portion of spent LIBs are recycled. In Australia, for example, only 6% of the 5290 tons of LIBs that reached end-of-life in 2017–2018 were used for recycling.[49] The spent LIBs of the NMC type with cathodes made of a combination of lithium, nickel, manganese and cobalt are recycled most often. Bhandari *et al.*[50] stated that recycling of NMC batteries is more economically justified than recycling of cheaper LFP batteries with a lithium ferro-phosphate cathode. This is due to the possibility of extracting not only lithium (as in LFP processing), but also nickel and cobalt in the case of NMC. According to calculations, the revenue from recycling of an NMC811 battery is more than three times higher than that from recycling of an LFP battery.[50]

Currently, there are three traditional methods for the recycling of spent LIBs, namely, pyrometallurgical, hydrometallurgical and combined processes. However, it is difficult to provide a constant supply of spent LIBs for a recycling plant; therefore, recycling is carried out with versatile process lines that use several types of batteries as the feedstock and yield a mixture of several products that can serve as the feedstock for another process.[49,51] In the pyrometallurgical processing of spent LIBs, lithium is not recovered, but is lost in slag and other waste.[45] More expensive cobalt and other metals are the target components in this case.[52]

Lithium can be recovered by hydrometallurgical techniques (Fig. 4). The spent LIBs are first discharged by immersion into a saline solution and then crushed; then the metallic components are removed. Graphite and polymers are separated by means of flotation. The hydrometallurgical process (evaporation and chemical precipitation) affords a lithium concentrate, from which Li_2CO_3 is extracted after filtration.

The estimates of the cost of lithium obtained from recycled LIBs are rather different.[14,50] Christmann *et al.*[14] reported that the cost of lithium obtained by recycling can be five times higher than the cost of lithium produced from natural brines. With that, according to recent analysis,[50] recycling of spent LIBs can give a significant income provided that the recovery efficiency is at least 90%, with the share of lithium being more than 50%.

3. Membrane-based methods for lithium recovery

3.1. Basics and concepts

According to the above flow diagram for lithium recovery (see Figs 2–4), a necessary stage is the separation of lithium from singly charged (monovalent) and multiply charged (multivalent) ions, especially Ca^{2+} and Mg^{2+} ions present

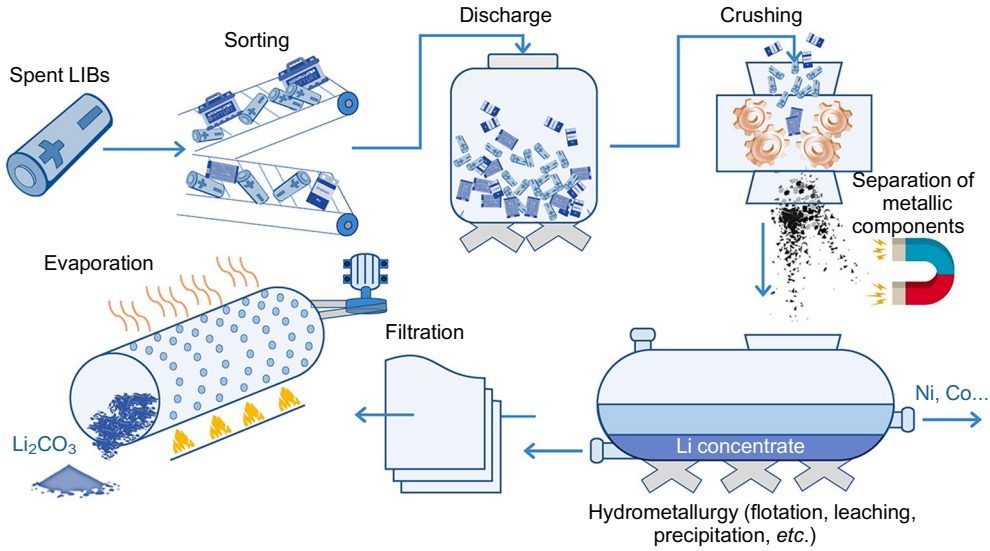

Figure 4. Flow diagram of the process of Li^+ extraction from spent LIB concentrate. The Figure was created by the authors using published data.[45]

in excess. The traditional hydrometallurgical approaches to separation (extraction, precipitation, filtration, *etc.*) are quite efficient and give products with a high degree of purity; however, these processes generate a large amount of waste water and are associated by relativly high energy and resource consumption.

A solution to this problem can come from the use of membrane separation methods included in combined process lines for the production of lithium and other valuable components. Membrane methods have already proved to be efficient in the production of potable and deionized water,[53–57] concentration of solutions,[58–60] recovery of industrial water components,[61] selective separation of ions,[61–63] energy production,[64,65] decarbonization of the economy,[66] *etc.*

The main advantage of membrane methods is low energy and material consumption. In addition, they almost do not require the use of chemicals. This significantly reduces the environmental burden from the use of hydrometallurgical methods, which cannot yet be completely abandoned (as shown below), at the stage of pretreatment of lithium-containing natural solutions. Nanofiltration (NF) and electrodialysis (ED) are most actively discussed in the literature as membrane methods promising for the extraction of lithium.

In the processing of natural lithium brines containing excess amounts of magnesium and calcium ions, the main difficulty is the selective separation of lithium. Many researchers note the importance of the magnesium to lithium ratio ($c_{Mg^{2+}}/c_{LI^{+}}$) in the brine, which largely determines the economically justified degree of lithium extraction. In the mined brine deposits, this ratio is, most often, in the range from <1 to 30,[67] but in some cases, it exceeds 100. In the latter case, the economic justification of brine processing becomes problematic.

The selectivity of transport of singly charged ions (Li^+) over doubly charged ions (Mg^{2+}) through an NF membrane or ion-exchange membrane (IEM) is characterized quantitatively using the permselectivity coefficient (or separation factor) $S_{Li^+/Mg^{2+}}$.[68,69]

$$S_{Li^+/Mg^{2+}} = \frac{j_{Li^+}/j_{Mg^{2+}}}{c^{f}_{Li^+}/c^{f}_{Mg^{2+}}} = \frac{\Delta c^{p}_{Li^+}/\Delta c^{p}_{Mg^{2+}}}{c^{f}_{Li^+}/c^{f}_{Mg^{2+}}} = \frac{P_{Li^+}}{P_{Mg^{2+}}} \quad (1)$$

where j_{Li^+} and $j_{Mg^{2+}}$ are flux densities of Li^+ and Mg^{2+} ions across the membrane; $c^{f}_{Li^+}$ and $c^{f}_{Mg^{2+}}$ are the concentrations of these ions in the feed solution; $\Delta c^{p}_{Li^+}$ and $\Delta c^{p}_{Mg^{2+}}$ are the changes in concentrations of these ions in the permeate (in the case of NF) or in the concentrate compartment (in the case of ED); P_{Li^+} and $P_{Mg^{2+}}$ are salt permeability coefficients [P_i (%)] of the membrane for the corresponding ion

$$P_i = \frac{c^{p}_i}{c^{f}_i} \times 100\% \quad (2)$$

The concentrations and fluxes appearing in Eqn (1) must be expressed in the same units indicating the amount of substance (moles or equivalents).

In the case of ion-exchange membranes, it is convenient to introduce the integral[70,71] (or effective[72,73]) transport numbers of ions in the membrane

$$T_i = \frac{z_i j_i \mathrm{F}}{J} \quad (3)$$

where z_i is the charge number of ion i, F is the Faraday constant, J is the electric current density. The flux density j_i may include electromigration, diffusion and convective components. The parameter T_i indicates the fraction of electric charge carried by ions i through the membrane under arbitrary conditions. Note that the classical (migration) transport number is measured under conditions where ions are transported only by electromigration.

The experimental fluxes of the competing cations (j_{Li^+} and $j_{Mg^{2+}}$) are determined from experimental quasi-stationary kinetic curves for the variation of cation concentrations in the feed or in the permeate (in the case of NF membranes), or in the concentrate (in the case of ED membranes). The ion fluxes can be found using the following equation:[74,75]

$$j_{Li^+} = \frac{V}{s}\frac{\mathrm{d}c_{Li^+}}{\mathrm{d}t} \quad (4)$$

where V is the volume of the feed or permeate (or concentrate) solution, s is the effective surface area of the membrane, t is time, c_{Li^+} is lithium ion concentration.

According to experimental and calculated results, pressure-driven membrane methods are effective for processing waters with high salinity (*e.g.*, for the processing of sea water with the salinity of $\sim$35 g L^{-1},[58,76,77]) while electrodialysis is used more often to process solutions with the salinity of up to 2.5–3.0 g L^{-1}, or more rarely, up to 15.0 g L^{-1}.[77]

3.2. General principles for the separation of monovalent and divalent ions using nanofiltration and electrodialysis

Typically, commercial membranes‡ for pressure-driven (baromembrane) processes such as reverse osmosis (RO) and nanofiltration can significantly reduce the concentrations of miltivalent ions (such as Ca^{2+} and Mg^{2+}) in the permeate compared to the monovalent ion concentrations. However, among all pressure-driven processes, only nanofiltration is suitable for separating miltivalent ions from monovalent ones, since only in this case, there is no significant decrease in the concentration of monovalent ions in the permeate. In the case of RO, the concentrations of all ions are reduced by 90–99%. In the case of widely used commercial NF membranes such as NF-90, DL, DK and NF-270 (Sterlitech, USA), the retention capability of the membrane for magnesium salt (salt rejection)

$$R_i = \left(1 - \frac{c^{p}_i}{c^{f}_i}\right) \times 100\% = (1 - P_i) \quad (5)$$

amounts to 60.5,[78] 65, 60[79] and 70.4%,[80] respectively. According to the manufacturer data,[81] R_{MgSO_4} for DL and DK membranes can reach 98 and 96%, respectively. However, the content of monovalent ions in the permeate also decreases by 40–50% (and even by 70%) relative to their content in the feed solution.[81–83] Thus, using commercial membranes, it is not always possible to achieve a significant separation of magnesium and lithium ions. In addition, in the resulting product solution, the concentration of the extracted lithium ion is significantly lower than in the feed solution.

‡ Hereinafter, the designations of membrane samples are trade names registered by manufacturers or names of non-commercialized (laboratory-made) membranes used in original publications.

A significant advantage of ED over NF is as follows: the competing ions from the initial solution can be not only separated, but also concentrated. However, the most common commercial sulfonate cation-exchange membranes selectively transfer divalent magnesium rather than monovalent lithium. This is attributable to stronger electrostatic attraction of doubly charged magnesium cations to the negatively charged ions present in the cation-exchange membranes compared to the attraction of singly charged lithium ions; this causes the preferential sorption of Mg^{2+} over Li^{+}.

The absence of effective NF and ED membranes for mono and divalent ion separation in the market encourages researchers to seek ways of membrane modification in order to increase the membrane ability to reject multivalent ions and transfer monovalent ions and thus to obtain high-purity products. An obvious way to modify commercial membranes with the goal to increase their efficiency in separating ions with different charge magnitudes is to coat the membrane surface with a thin layer containing ions with a charge opposite to the charge of the ions present in the pristine (substrate) membrane (Fig. 5 *a*).[84] In this case, multivalent ions that pass through the modifying layer will experience a much greater electrostatic repulsion than monovalent ions. In other words, the modifying active layer serves as a barrier for competing ions, and the greater the ion charge, the higher the barrier.

Using surface modification, it is possible to fabricate NF and ED membranes with relatively high monovalent ion selectivity. A higher selectivity can be achieved by using alternating deposition of layers with oppositely charged fixed ions. This procedure is called layer-by-layer (LbL) deposition (Fig. 5 *b*).

Monovalent-ion permselectivity of membranes can also be attained by other approaches. The active surface layer can be made selective if it has a high degree of cross-linking. This creates steric hindrance for ions with a relatively great hydrated radius such as multivalent cations (sieve effect[85, 86]). Early applications of ion-exchange membranes (IEMs) modified in this way were aimed at increasing the Na^{+} transport selectivity in the production of table salt from sea water.[68]

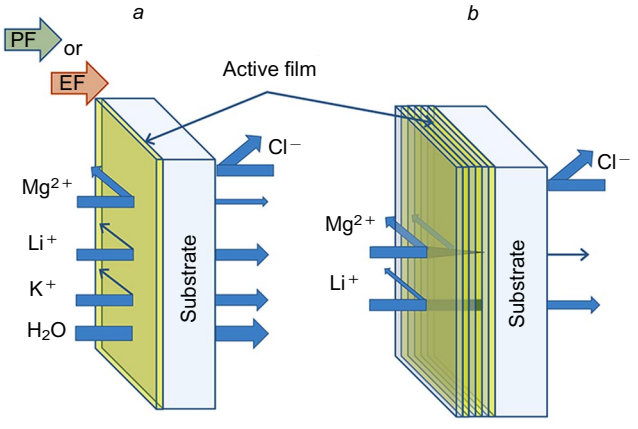

Figure 5. Diagram of ion separation using bilayer- (*a*) and multilayer (*b*) membranes in baromembrane and electromembrane processes under the action of pressure field (PF) or electric field (EF), respectively. The substrate membrane suppresses the electromigration of co-ions (in this case, anions). The thin active film serves as a barrier for cations; the barrier for divalent cations is much higher than that for monovalent cations. In the case of an NF membrane, the water flux through the membrane much exceeds the ion fluxes, which results in a permeate being a more dilute solution than the retentate. During ED, the water flux through the membrane is many orders of magnitude lower than that in NF.

A dense polymer layer with a low constant charge deposited on the membrane can also serve as a barrier to highly hydrated multivalent ions with a high degree of hydration. An example of such polymer is polypyrrole, which has an extremely dense and rigid structure and high hydrophobicity and thus provides a significant specific monovalent ion selectivity of a bilayer membrane.[87] One more polymer suitable for this type of modification is polyethyleneimine (PEI). Modification of anion-exchange membranes with a polyethyleneimine layer provides a relatively high monovalent ion selectivity, although the stability of this layer over time is moderate.[88–90]

A lot of attention of specialists is paid to increasing the stability of the fabricated structures. This is attained by fairly intricate approaches. With the goal of increasing the reactivity of substrate membrane surface, Zhang *et al.*[91] coated the membrane surface with PEI and chitosan using polydopamine. In the next stage, they coated the substrate membrane with reactive blue 4 dye containing sulfonate groups by electrodeposition. The dye reacted with the amino groups of the anion-exchange membrane and hydroxyl groups of chitosan to form strong covalent bonds. The negatively charged sulfonate groups served to create a barrier to multivalent anions, thus providing permselectivity to monovalent anions.

3.3. Selective extraction of lithium using porous membranes in pressure-driven processes. Efficient methods for modifying nanofiltration membranes

This part of the review addresses recently developed methods for efficient modification of filtration membranes to provide for the selective transfer of monovalent cations. Many commercial porous membranes for RO and NF (*e.g.*, those made from polyether imide, polysulfone, polypiperazine and other polymers) contain negatively charged groups (carboxyl or sulfonate groups). A change in the sign of the membrane surface layer charge from negative to positive makes it possible to enhance the Donnan exclusion effect for cations, especially for divalent cations, thus increasing the monovalent ion selectivity of the modified membranes.[92, 93]

Grafting of polyethyleneimine (PEI) with a variable molecular weight to a large-pore substrate showed higher performance for the membrane pretreated with a low-molecular-weight PEI compared with that pretreated with a higher-molecular-weight PEI.[92] Lu *et al.*[92] attributed this result to the fact that in the presence of low-molecular-weight PEI, the steric hindrance for polymer contact with the membrane surface decreases, resulting in generation of a higher positive charge density and a tighter structure of the modifying agent (Fig. 6).

Modification of the membrane surface with the most beneficial low-molecular-weight PEI (MW = 600) led to a relatively high selectivity for the separation of lithium and magnesium ions ($S_{Li^+/Mg^{2+}} \approx 8.0$) and relatively high lithium flux in the membrane (Table 1).

One more method for increasing the selectivity of separation of competing ions is to generate conditions for specific interactions of one of the ions (or a group of ions in the solution) with the membrane. It was established that NF membranes modified with positively charged PEI molecules demonstrated higher selectivity after contact with negatively

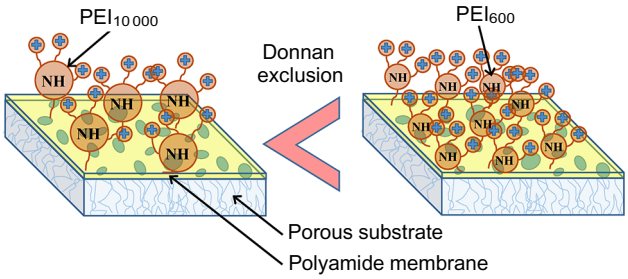

Figure 6. Scheme illustrating the effect of the molecular weight of grafted polyethyleneimine on the permselectivity of commercial membranes.

charged ethylenediaminetetraacetate (EDTA) molecules.[97] Even a low EDTA concentration (2–3 mass %) led to an increase in the Mg^{2+} rejection by ~30%, which is probably due to the adsorption of Mg^{2+} on the EDTA-modified surface.[97]

Apart from the good separation capacity of the membrane, high water permeability coefficient of the membranes is also of great importance. Zhang *et al.*[83] described a modification method of a commercial polyether sulfone (PES) ultrafiltration membrane, which involved deposition of multiwalled carbon nanotubes (CNTs) grafted with piperazine. After the introduction of CNTs, the water permeability of the modified membrane increased up to 14.0 L $(m^2\ h\ bar)^{-1}$, while salt rejection of $MgCl_2$ improved from 94.2 to 96.9%. According to our estimates, the separation factor between Li^+ and Mg^{2+} was ~25.

Ni and co-workers[94,95] also used CNTs as a binding agent for subsequent grafting of piperazine. The incorporation of multiwalled CNTs functionalized with polyethyleneimine into a commercial substrate membrane provided a high selectivity to lithium ($S_{Li^+/Mg^{2+}} = 60$),[95] while the rejection coefficients for magnesium and lithium reached 98.5 and 11.5%, respectively. Thus, the monovalent ion selectivity is mainly due to reversal of the surface charge of a commercial membrane from negative to positive as a result of the presence of amino groups in the modifying polymer. Also, CNTs are necessary to ensure high water permeability of the membranes [~11.5 L $(m^2\ h\ bar)^{-1}$ for the modified membrane].

High membrane permselectivity can also be attained by forming carboxylated cellulose nanocrystals in the modifying layer. Guo *et al.*[96] developed and studied a composite three-layer membrane based on the PES substrate membrane coated with a negatively charged layer of carboxylated cellulose nanocrystals and a positively charged polyamide layer. The Janus structure gave rise to a large difference between the retention capability for Mg^{2+} and Li^+ in a model brine with high $Li^+ : Mg^{2+}$ mass ratio. Owing to the thin layer of polyamide, it was possible to achieve a relatively high water permeability coefficient of 3.4 L $(m^2\ h\ bar)^{-1}$.

Outstanding results in the Li^+ and Mg^{2+} separation were achieved by modification of a commercial NF membrane by self-polymerization of polydopamine followed by grafting of PEI to introduce amino groups onto the membrane surface.[80] A high separation factor ($S_{Li^+/Mg^{2+}} = 60$) at a rather high water permeability coefficient [3.4 L $(m^2\ h\ bar)^{-1}$] was found for this membrane. The

Table 1. Efficiency of NF membranes with a modified positively charged active layer for the separation of Li^+ and Mg^{2+}.

Designation of the membrane sample [a]	P, bar	c_i^f, g L^{-1}	$c_{Mg^{2+}}/c_{Li^+}$ (see [b])	R_i (%)	$S_{Li^+/Mg^{2+}}$	Water permeability, L $(m^2\ h)^{-1}$	j_i, mol $(m^2\ h)^{-1}$ (see [c])	Ref.
MWCNTs-OH/PIP	4	0.022 0.470	20	20 97	25.0	34.0	7.1×10^{-4} 1.7×10^{-4}	83
PES UF/GO-doped,	3	0.023 0.470	20	20.9 95.1	16.0	33.6	4.8×10^{-3} 1.7×10^{-3}	94
PES-MWCNTs-COOK/PEI-TMC	3	0.022 0.470	20	11.5 98.5	60.0	34.5	4.2×10^{-4} 4.0×10^{-3}	95
SP_E-PEI600	6	3.3×10^{-3} 0.5	150	22.5 90.5	8.0	24.2 32.5	0.053 [d] 0.380 [d]	92
PEI/TMC/CNC-COOH	8	8.2×10^{-3} 0.5	60	11.6 95.6	5.8	27.2	– –	96
PA-B2-E3	10	0.1 2.4	24	15.1 91.9	12.7	6.0	2.0×10^{-3} 1.3×10^{-3}	97
PDA-PEI DK	6	0.4 11.6	30	16.0 98.6	60.0	21.3	– –	80
DAIB	6	0.082 2.5	30	55.6 95.8	11.1	64.8	0.70 [e] 0.56 [e]	98
QEDTP NF	6	4.0×10^{-3} 0.5	120	31 95.6	15.6	126.9	7.0×10^{-4} 1.5×10^{-3}	79

Note. For c_i^f, R_i and j_i, the values above the line refer to Li^+ ions and those below the line correspond to Mg^{2+} ions. [a] The designations for experimental membrane samples used in original publications are given. [b] Mass ratio. [c] We determined the lithium and magnesium fluxes through the membranes by calculations based on published data. [d] The calculations were performed using additional data kindly provided by the authors of Ref. 92. [e] The values were reported in Ref. 98; it was impossible to verify the results using the reported data.

lithium flux across the membrane was more than five times higher than the magnesium flux.

Modification of a commercial polyamide NF membrane using a bis-quaternary ammonium salt furnished a loose structure of the modifying layer with a low hydraulic resistance.[79] The membrane had an excellent water permeability coefficient [21.1 L (m^2 h bar)$^{-1}$] with high $MgCl_2$ (R_{MgCl_2} = 95.6%) rejection when tested in brine with $c_{Mg^{2+}}/c_{Li^+}$ = 120.

Thus, the main trends in the improvement of NF membranes for the selective extraction of lithium are related to both increasing rejection of magnesium and increasing the water permeability. The commercial counterparts of these membranes are governed by the well-known permeability/selectivity trade-off: a membrane with high permeability usually has low selectivity and *vice versa*.[63]

However, it should be noted that despite the fact that the above modified filtration membranes usually exhibit high $MgCl_2$ rejection and high separation factors, the flux of Mg^{2+} ions across the membrane is still rather high, being often comparable to or even higher than the Li^+ flux due to the high $c_{Mg^{2+}}/c_{Li^+}$ ratio (see Table 1). The two-stage separation of a lithium and magnesium mixture ($c_{Mg^{2+}}/c_{Li^+}$ = 50, salt content c_{tot} = 25.5 g L^{-1})[98] using a positively charged membrane decreased the $c_{Mg^{2+}}/c_{Li^+}$ ratio from 50 to 8.75 in the first NF cycle and to 0.85 in the second cycle. However, an increase in the number of filtration cycles resulted in high loss of the target Li^+ ions.

Attempts to separate more complex mixtures (containing more than two competing ions) are less successful. The separation factors for the same Li^+ and Mg^{2+} pair decreases from 25 to 4 in the presence of Na^+ and Ca^{2+} ions.[83] Note that membranes of this type do not exhibit specific selectivity in a mixture of singly charged ions. In addition to Li^+, they are equally permeable for Na^+ and K^+, which are more abundant in natural brines than Li^+.

The characteristics attained by recently developed NF membranes used for the selective recovery of lithium are summarized in Table 1. Note that some of the lithium and magnesium fluxes across the membrane presented in the Table are our own estimates derived from the data reported in original publications; these estimates may be rough. The ion fluxes were calculated using the values of the permeate/water flux, the concentrations of the respective ions in the permeate and the time of the experiment.

Despite the high selectivity of some NF membranes described in this Section, the flux density of lithium ions across the membranes is relatively low, being mainly in the range of $10^{-4}-10^{-3}$ mol (m^2 h)$^{-1}$. An exception is the SP_E-PEI_{600} membrane;[92] in this case, at a very low Li^+ concentration in the feed solution (3.3×10^{-3} g L^{-1}), a relatively high flux was obtained [0.053 mol (m^2 h)$^{-1}$]. Peng and Zhao[98] also reported a relatively high flux of Li^+ ions through DAIB membrane [0.7 mol (m^2 h)$^{-1}$ at the 0.082 g L^{-1} concentration in the feed solution]; however, an alternative calculation of the results presented by the authors was impossible.

3.4. Lithium extraction using ion-exchange membranes *via* electromembrane processes

3.4.1. Design features of monovalent-ion permselective ion-exchange membranes

Electromembrane processes such as electrodialysis (ED) and membrane electrolysis seem to be the most promising for ion separation on an industrial scale, as these processes achieve both high selectivity and high permeation rates for the preferentially transferred ions.

In the case of ion-exchange membranes, it is conventional to distinguish the selectivity between counter-ion and co-ion transport (counter-ion permselectivity)[99] and selectivity between two different counter-ions (permselectivity for specific ions).[100] The counter-ion permselectivity of IEMs is due to the electrostatic interactions between the mobile ions and functional groups present in the membrane matrix, with counter-ions being drawn into the matrix and co-ions being pushed away by electrostatic forces. This feature enables efficient desalination and concentration of electrolyte solutions.[58] The permselectivity for specific ions makes it possible to separate/extract specific ions from mixed solutions. As in the case of modified NF membranes described in the previous Section, highly selective separation is possible only if the ions to be separated have different charge magnitudes (monovalent and multivalent ions).

Like pressure-driven processes, electromembrane processes make it possible to effectively extract lithium in the presence of excess magnesium (up to $c_{Mg^{2+}}/c_{Li^+}$ = 300).[101] However, the flux density of lithium across IEM decreases with increasing $c_{Mg^{2+}}/c_{Li^+}$ ratio in the feed solution.

In the case of some cation-exchange membranes (containing sulfonic groups in the surface layer), the divalent counter-ions can be specifically (in an amount higher than equivalent) adsorbed on these groups under the action of an external electric field (Fig. 7). This type of adsorption was discussed in several publications;[102–104] this effect is enhanced when electric current is passed.[105] The adsorption of calcium and/or magnesium ions gives rise to a positively charged layer on the membrane surface; this layer generates a local electrostatic repulsive force acting on cations, which prevents them from entering the membrane.[101,105] However, this barrier acts on both multiply and singly charged ions, and it is much stronger for the multiply charged ions. Upon an increase in the $c_{Mg^{2+}}/c_{Li^+}$ ratio,[101] current density, and the time of current flow,[105] the density of the positive electric charge on the membrane surface increases, causing an increase in the separation effect and in the $S_{Li^+/Mg^{2+}}$ permselectivity.[101]

As in the case of NF membranes, it is fairly efficient to modify IEMs with polymer films containing functional groups with a charge opposite to that of the substrate membrane (see Fig. 5). Using this approach, it is possible

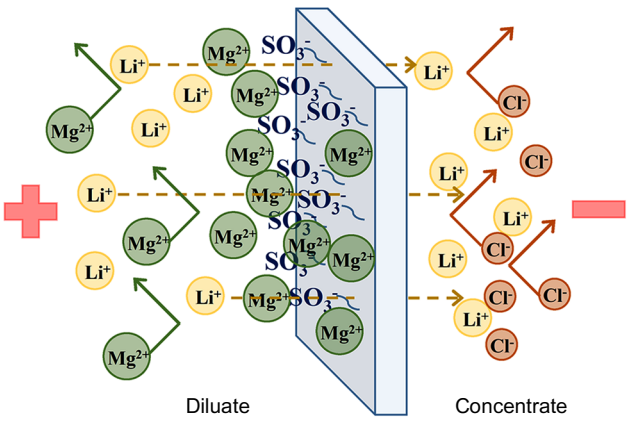

Figure 7. Formation of a positively charged layer of Mg^{2+} cations on the surface of a cation-exchange membrane.

to achieve a significant monovalent-ion permselectivity. A more pronounced effect can be achieved by LbL deposition of a large number of polymer layers with alternating fixed charges; however, the resistance of the membrane also increases. The LbL deposition of polymers for membrane modification has been successfully used for both IEM membranes [106–109] and NF or RO membranes.[110, 111]

3.4.2. Lithium extraction using commercial ion-exchange membranes

The most popular commercial monovalent-ion permselective anion- and cation-exchange membranes are Neosepta AMS, CMS, ACS, CIMS, Selemion ASV, CSO, Fumasep FAA, FKL and FKE. These membranes have a structured surface layer that rejects multivalent ions with large hydration shells. The multivalent ion rejection is attained using a variety of approaches: deposition of a highly cross-linked surface layer (this is done in Neosepta CMS [112]) or an oppositely charged layer (*e.g.*, the Selemion CSO cation-exchange membrane contains a thin polyethyleneimine anion-exchange surface layer [113, 114]).

The use of the above-mentioned commercial membranes in the selective electrodialysis (S-ED) makes it possible to attain a relatively high separation selectivity for lithium. The configuration of repeating (elementary) unit for S-ED is the same as that for conventional ED. The separation of lithium and magnesium ($c_{Mg^{2+}}/c_{Li^+} = 150$, $c_{Li^+} = 0.15$ g L^{-1}) with the Selemion CSO cation-exchange membrane resulted in $S_{Li^+/Mg^{2+}}$ of 33;[101] according to our calculations, the lithium flux was 0.17 mol (m^2 h)$^{-1}$. It should be taken into account that during desalination in the batch recycle mode, the concentration of lithium in the feed solution decreases and, hence, the lithium flux through the cation-exchange membrane also decreases. Ying *et al.*[115] showed that ~3 h after the start of the batch recycle electrodialysis desalination of a mixture containing ~8 g L^{-1} of Li^+ ($c_{Mg^{2+}}/c_{Li^+} = 9.85$), the recovery rate of lithium on a Selemion CSO membrane was 90% (in Fig. 8, the time corresponding to this recovery rate is marked by a vertical dashed line). At a constant current density of 140 A m^{-2}, the lithium flux through this membrane decreased from the initial value of ~3.5 mol (m^2 h)$^{-1}$ to 1.0 mol (m^2 h)$^{-1}$ after 2.5 h (Fig. 8 *a*). The Mg^{2+} flux increased with time and became comparable with the Li^+ flux at the end of the process.

The efficiency of energy utilization decreased rapidly with decreasing content of lithium in the feed solution (Fig. 8 *b*); therefore, to attain lithium recovery rate above 90%, a significant increase in the energy consumption is required. Nevertheless, it is possible to decrease the $c_{Mg^{2+}}/c_{Li^+}$ ratio from 9.85 to 0.57.

Zhang *et al.*[116] showed that the continuous feed and bleed mode is more efficient for S-ED than the batch recycle mode. In this case, the concentration of the feed solution circulating through the desalination chamber of the electrodialysis cell is maintained constant by adding new portions of the feed solution and withdrawal of a part of the desalinated solution. Indeed, the separation factor for lithium and magnesium ions (for the initial mixture, $c_{Mg^{2+}}/c_{Li^+} = 60$, $c_{Li^+} = 0.26$ g L^{-1}) with a CIMS membrane increases from 4.6 (batch recycle mode) to 11.5 (feed and bled mode), and the current efficiency increases from 1.7 to 9.0%; this opens up prospects for the industrial application for the latter process.

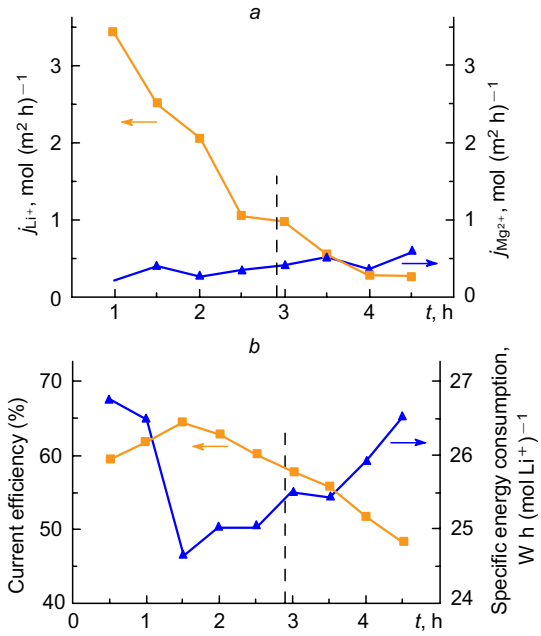

Figure 8. Time variations of the flux density of Li^+ and Mg^{2+} ions (*a*), current efficiency and specific energy consumption (*b*) in the batch recycle mode of the electrodialysis separation of a mixed solution.[115] Published with permission from Elsevier.

Another important problem is the presence of various competing ions in real feed solutions. Ji *et al.*[117] studied the effect of the concentrations of accompanying cations, Na^+, K^+, Ca^{2+}, and Mg^{2+}, on the separation of Mg^{2+} and Li^+. High concentrations of the interfering cations have an adverse effect on the lithium flux in S-ED; the effect decreases in the following order of cations:

$$K^+ > Na^+ > Ca^{2+} > Mg^{2+}$$

When the c_{Na^+}/c_{Li^+} ratio in the feed solution supplied to the desalination chamber increases from 1 to 20, the separation factor between magnesium and lithium determined from the change in the component concentrations (Δc_i^f) in the desalination chamber,

$$S_{Mg^{2+}/Li^+} = \frac{\Delta c^f_{Mg^{2+}}(t = x)/\Delta c^f_{Li^+}(t = x)}{c^f_{Mg^{2+}}(t = 0)/c^f_{Li^+}(t = 0)} \quad (6)$$

decreases from 8.7 to 1.8. This is attributed to the fact that Mg^{2+} ions are poorly transported through a monovalent-ion permselective cation-exchange membrane and their flux is weakly dependent on the presence of sodium. Meanwhile, the lithium flux sharply decreases upon the addition of Na^+, since sodium is transported through the monovalent-ion permselective membrane equally well and hence actively competes with Li^+. The S_{Mg^{2+}/Li^+} ratio changes in a similar way when K^+ ions are added to the feed solution: when the c_{K^+}/c_{Li^+} ratio increases from 1 to 20, the S_{Mg^{2+}/Li^+} value decreases from 8.3 to 2.1. In other words, on going from a solution containing only lithium and magnesium to a mixed solution resembling natural water in the qualitative composition, Mg^{2+} ions are still effectively rejected by the monovalent ion-selective IEM; in this case, not only Li^+ ions, but all singly charged cations are easily transported through the membrane; as a result, the transport number of lithium ions in the membrane sharply decreases.

Thus, using S-ED, it is possible to efficiently reduce the Mg^{2+}/Li^{+} ratio in the feed solution with a high magnesium concentration; the compounds do not undergo phase transitions, and the method is characterized by low energy consumption. The latter varies over a wide range, but the range of minimum values is $\sim 0.01-0.2$ kW h (mol Li^{+})$^{-1}$. The variations in the energy consumption are determined by the chemical composition of the treated solutions. For example, if the lithium ion concentration in the feed solution is high and the concentration of multiply charged ions is low, then the energy consumption is relatively low [0.025 kW h (mol Li^{+})$^{-1}$] and the current efficiency is high (50–90%).[115,118] Otherwise, the current efficiency for lithium ions is low ($\sim 1-10$%), and to attain a reasonable performance, high current density is required. Naturally this leads to higher energy consumption [up to 1.6 kW h (mol Li^{+})$^{-1}$ (Ref. 116)], calling into question the economic feasibility of processing of such solutions.

It should also be emphasized that S-ED with commercial IEMs does not enable the separation of ions with the same charges (such as Li^{+} and K^{+}).[117] This method can only concentrate these ions,[118] for the subsequent use of precipitation or other techniques for the selective extraction of lithium compounds. However, despite the difficulties, the use of S-ED can greatly simplify the traditional process flow diagram and has good prospects for industrial application.

Most of the publications on the extraction of lithium by means of IEMs are focused on the use of electrodialysis for the processing of brines (more commonly, artificial solutions that are simplified models of natural brines). A much smaller number of publications address the use of this process to recover lithium from ore leachates. Zhou *et al.*[119] investigated parameters for concentrating a lithium-containing solution obtained from lithium ores using three types of commercial membranes. The estimates of average ion flux and energy consumption showed that a pair of the Neosepta AMX/CMX membranes was more suitable for concentrating than FKS/FAS and CJMC/CJMA membranes.

Martin *et al.*[120] proposed a flow diagram for the extraction of lithium as Li_2CO_3 from the zinnwaldite mineral. A lithium-containing extract ($c_{Li^+} \approx 0.3$ g L^{-1}) was obtained by CO_2/water treatment of the ore at 100 bar and 230 °C. After a number of additional processing and filtration stages, a solution containing lithium bicarbonate was obtained. Then it was concentrated by electrodialysis up to a lithium content of 8.5 g L^{-1}. The authors stated that the use of monovalent-ion permselective Neosepta CMS membranes makes it possible to remove up to 90% of multivalent ions, with the concentrate being enriched in Li^{+}, K^{+} and Rb^{+} ions. The concentrate containing $LiHCO_3$ was heated to 90–95 °C in order to remove CO_2 and obtain Li_2CO_3. According to authors estimates, this process provides lithium carbonate with a purity above 99.0% without additional rinsing.

In addition, S-ED has been successfully used to process leach solutions from spent lithium-ion batteries.[121–125] The rate of lithium extraction in the processing of leach solutions of NMC111 cathode materials using this method was ~ 3.0 mol (m^2 h)$^{-1}$; the permselectivity coefficient for lithium over other cations present in the solution (Ni^{2+}, Mn^{2+} and Co^{2+}) amounted to 5.[122] Combining complex formation with a three-stage S-ED process makes it possible to separately recover lithium, nickel, manganese and cobalt with a >99% purity.[121] In some cases, the purity of the extracted Li_2CO_3 was very high (99.6%) and corresponded to battery grade.[125]

Meanwhile, the extracts of ores and spent batteries and also natural brines require pretreatment before being fed into the electrodialysis cell. A combined process including reverse osmosis and electrodialysis appears to be most promising for the industry. Qiu *et al.*[118] evaluated the economic feasibility of using RO together with S-ED. Lithium-containing waste water ($c_{Li^+} \approx 1.27$ g L^{-1}; specific conductivity of 17.9 mS cm^{-1}) was preconcentrated by reverse osmosis (to increase the initial concentration $\sim$3-fold), and then RO retentate was used as a feed solution for S-ED on CIMS and ACS membranes. The energy consumption at the RO stage was ~ 0.2 kW h (mol Li^{+})$^{-1}$, which corresponded to 7.81 kW h per m^3 of waste water. The energy consumption for the processing of RO retentate (with electrical conductivity of 55 mS cm^{-1}) by ED may amount to ~ 0.12 kW h (mol Li^{+})$^{-1}$. This corresponds to 32.6 and 7.71 kW h per m^3 of the feed solution for the first and second S-ED stages, respectively. The final concentrate may contain up to 87 g L^{-1} of LiCl. The estimated cost of lithium chloride obtained by S-ED from a preconcentrated solution may be markedly lower than that for the reagent-based methods.[118]

3.4.3. Design of novel monovalent-ion permselective membranes for Li^{+} extraction using electrodialysis

Although monovalent-ion-permselective IEMs are commercially available, these special-grade membranes are more expensive than the conventional ion-exchange membranes. Meanwhile, the internal logic of science stimulates the search for new, more efficient membranes. The efforts of many of laboratories throughout the world are focused on the development of more efficient monovalent-ion permselective IEMs;[126] this is reflected in increasing number of publications on this subject. Some new trends in the development of this type of IEMs for electrodialysis are described below.

Surface modification is widely used for improving membrane properties and performance without significantly increasing their cost. In particular, this approach is actively utilized to improve conventional ion-exchange membranes, in order to achieve a high permselectivity in the separation of solution components. Therefore, a lot of attention in membrane science is paid to the search for modification methods for inexpensive commercial IEMs or to design of new membranes with a specific structure increasing the permselectivity for particular ions.[68,87,107,127–129] Currently, permselectivity is increased using a number of approaches such as LbL deposition,[106,109,130] polymer blending,[131] covalent cross-linking,[132,133] electrospinning[134] and preparation of organic-inorganic composite materials.[85,135,136]

Zhao *et al.*[137] reported a highly selective separation attained for Li^{+}/Ca^{2+} and Li^{+}/Mg^{2+} pairs ($S_{Li^+/Mg^{2+}} = 8$ and 15, respectively) using composite cation-exchange membrane made by LbL assembly (the best result was obtained for 5.5 layers). In the case of hybrid membranes based on polyvinyl alcohol modified with one cationic and two anionic layers,[138] the Li^{+}/Mg^{2+} permselectivity coefficient was 5.2. This result is comparable with the result attained using NF membranes (see above).

However, separation of monovalent ions is a much more challenging problem. The use of commercial IEMs (and sometimes even specially designed laboratory IEMs[137,139])

does not provide a significant decrease in the flux of sodium ions compared to lithium; hence, the permselectivity coefficient between these ions calculated by Eqn (1) does not differ much from unity.

High permselectivity for lithium may be inherent in composite polymer and organic/inorganic hybrid membranes with additional introduced materials: sorbents, ionic liquids, porous inorganic additives, *etc.*[139–145] Hoshino[146] proposed lithium ion-conducting glass ceramics (ceramic material used in LIBs) to fabricate membranes selectively permeable to Li^+ and thus to extract lithium from sea water. Ounissi *et al.*[147,148] prepared a lithium-selective composite membrane by the introduction of lithium ion-conducting glass ceramic powder together with a non-ionic surfactant (BRIJ76) into an anion-exchange polymer (polyepichlorohydrin quaternized with 1,4-diazabicyclo[2.2.2]octane copolymerized with amino-polyethersulfone). This membrane demonstrated a very high selectivity for lithium ($S_{Li^+/Na^+} = 112$) in the ED desalination of a mixture of lithium and sodium ($c_{Na^+}/c_{Li^+} = 10$, $c_{tot} = 2.2$ g L^{-1}). Thus, a highly selective laboratory ion-exchange membrane was obtained for the first time, capable of recovering lithium not only from its mixed solutions with multivalent cations, but also from solutions with monovalent cations.

Zhao *et al.*[140] studied a composite sandwich membrane consisting of two cation-exchange membranes and tri-n-butyl phosphate (TBP) ionic liquid sandwiched between them. This approach to membrane modification with the goal of increasing the selectivity has already been known;[149–151] it is based on the fact that the organic phase contains a carrier (an organic extracting molecule) that selectively binds to the target metal ion. These carriers are capable of forming lipophilic organometallic ligands, which are then transported across the deposited organic phase *via* diffusion or electromigration. The target ion is released in the receiving phase (Fig. 9). The release of lithium becomes possible owing to the use of highly concentrated HCl as the receiving solution. Theoretically, it is possible to attain an exceptionally high selectivity using this method, since among all cations present in the feed solution (Li^+, Na^+, K^+, Mg^{2+}, Ca^{2+}), only Li^+ ions should react with the carrier ligands and be transferred through the selective layer. According to experiments,[140] no K^+ or Ca^{2+} ions were present in the concentrate, and according to our estimates, the permselectivity coefficient for Li^+ over Na^+ was ~10.

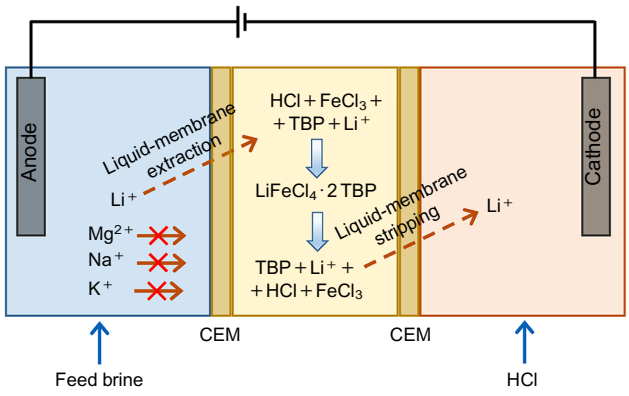

Figure 9. Schematic diagram of the lithium transfer in a multilayer liquid membrane used in electrodialysis.[140] CEM is cation-exchange membrane.

A membrane made of vermiculite flakes assembled into 2D layers, proposed by Razmjou *et al.*,[152] demonstrated selective transfer of Li^+ ions over Na^+ and K^+ ions, with separation factors being 1.3 and 1.6, respectively. The composite membrane consisting of graphene oxide nanosheets with ZIF-8 zeolite crystals deposited on an anodic alumina substrate by spin-coating to produce an ultrathin seeding layer showed S_{Li^+/Na^+} and S_{Li^+/K^+} values of 1.4 and 2.2, respectively.[153]

Sharma *et al.*[154] proposed a composite cation-exchange membrane based on sulfonated poly(ether ether ketone) and magnesium-doped lithium manganese oxide. Lithium ions were selectively transferred across the membrane *via* electromigration; the lithium flux was 4.3 mol $(m^2\ h)^{-1}$ and $S_{Li^+/Na^+} = 2.2$, $S_{Li^+/K^+} = 3$.

3.4.4. Electrodialysis with bipolar membranes and electrolysis with ion-exchange membranes

Electrodialysis with bipolar membranes (EDBM) is one more technique suitable for extraction of lithium from solutions.[155,156] Using bipolar membranes, it is possible to generate H^+ and OH^- ions without addition of reagents and to recover lithium as LiOH. Natural lithium-containing brines may serve as feed solutions. In this case, the final concentrate contains, in addition to Li^+ ions, also Na^+ and K^+ ions, which are present in natural brine.[157] It should be emphasized that in the EDBM process, like in the case of S-ED, the lithium flux, the recovery rate and the purity of lithium product are determined by characteristics of the used monovalent-ion permselective IEM. In the presence of competing Na^+ and K^+ cations, the Li^+ ion flux regularly decreases and specific energy consumption for the production of LiOH increases.[157] Owing to their higher mobility, K^+ ions have a more pronounced negative effect than Na^+ ions ($S_{Li^+/Na^+} = 0.7$ and $S_{Li^+/K^+} = 0.5$).

A considerable advantage of EDBM is the possibility of simultaneous formation of acid and base solutions in different chambers of the electrodialysis cell. This can be used to produce separate solutions enriched in cations and/or anions of valuable elements from the feed solution. In particular, EDBM was successfully utilized to separate boron and lithium.[158,159] Boron compounds are used to produce glass and ceramics, detergents, fertilizers, *etc.* While getting in the chamber confined by monopolar cation- and anion-exchange membranes, lithium present in the feed solution (boron, 0.8 g L^{-1}; lithium, 0.25 g L^{-1}) is transported through the cation-exchange membrane and reacts with OH^- ions generated by the bipolar membrane. Meanwhile, boron, which is present in the feed solution as the $B(OH)_4^-$ borate anion, is transported through the anion-exchange membrane, reacts with H^+ ions generated by another bipolar membrane and thus remains in the chamber as boric acid. The removal of lithium and boron amounts to 99 and 74%, respectively.[158]

The H^+ and OH^- ions can be generated not only using bipolar membranes, but also with electrodes. Both EDBM and electrolysis with IEMs are economically feasible.[160,161] Lithium can be selectively extracted using a three-stage process:[161]

— in the first stage, Mg^{2+} and Ca^{2+} ions are removed from the solution as $Mg(OH)_2$ and $Ca(OH)_2$ precipitates formed upon the reactions of these ions with OH^- anions generated at the cathode;

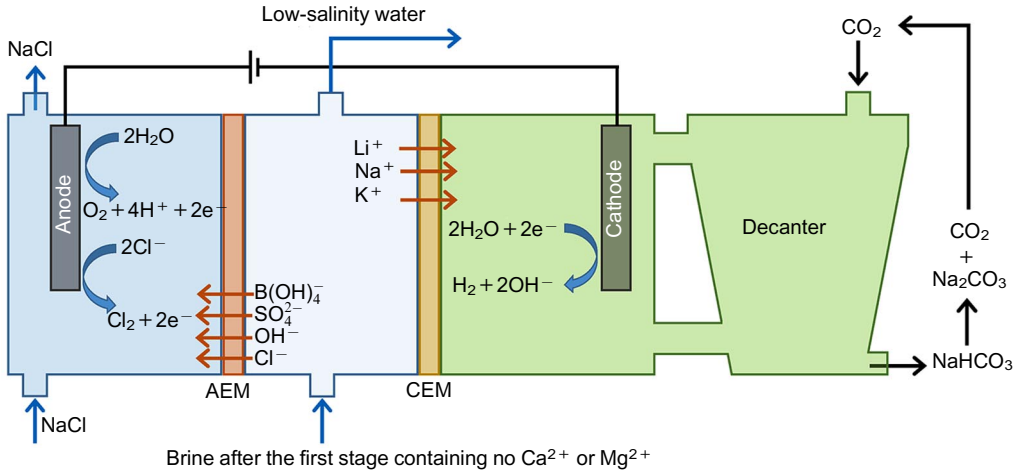

Figure 10. Schematic diagram of the second stage of Li_2CO_3 production: selective separation of Na^+ ions from natural solutions by electrolysis.[161] AEM is anion exchange membrane.

— in the second stage, Na^+ cations are recovered as the solid Na_2CO_3 precipitate with 99.5% purity (Fig. 10); sodium ions can be extracted from a mixture of singly charged ions (Na^+, Li^+ and K^+) owing to higher transport numbers of Na^+ ions in the membrane compared to the transport numbers of Li^+ or K^+;

— in the third stage, lithium carbonate is extracted in a similar way.

The amount of Na^+ ions transferred through the cation-exchange membrane in the second stage can indeed be many times greater than the amount of Li^+ ions if the sodium concentration in the solution entering the membrane electrolyzer significantly exceeds the lithium concentration (Na^+ concentration $\approx$115, K^+ concentration $\approx$16 and Li^+ concentration $\approx$1.3 g L^{-1}).[161] At 50 °C, the solubility of sodium carbonate is 47 g per 100 g of H_2O and that of lithium carbonate is 1 g per 100 g of H_2O.

Thus, the described electrically driven processes, in contrast to pressure-driven processes, make it possible not only to separate monovalent ions from multivalent ions, but also to separate ions of the same charge, *e.g.*, to extract lithium from a mixed solution of singly charged cations. These methods can form a reagent-free alternative to some stages of the hydrometallurgical production of lithium from primary and secondary sources.

4. Theoretical aspects of ion separation using nanofiltration and electrodialysis membranes

4.1. General equations and main assumptions

As noted above, monovalent ion-selective NF membranes have a thin active layer deposited on a porous substrate.[162] The active layer thickness is in the range of 5–200 nm,[163–165] and the pore diameter in this layer is $\sim$1 nm.[166, 167] Monovalent-ion permselective IEMs for electrodialysis have a similar design.[68, 107] The monovalent-ion permselectivity can also be ensured by a thin active layer (or layers). However, conventional IEMs meant for preventing the co-ion transport rather than porous membranes are used as substrates. Biesheuvel *et al.*[168] noted that the desalination and transport mechanisms in NF/RO and ED systems are very different, but, nevertheless, thorough analysis shows that they have much in common in the physical and chemical aspects,[71, 169] and, hence, in their mathematical description. The following mechanisms contributing to the monovalent-ion permselectivity of NF membranes are distinguished: Donnan exclusion of co-ions, steric hindrance and dielectric exclusion.[166, 170–175] The concentration of co-ions in the pore space of the membrane largely determines the membrane selectivity to the transfer of counter-ions. The steric hindrance can affect the mobility of competing counter-ions in different ways. The dielectric exclusion is usually neglected in the descriptions of the competitive transport through IEMs; usually, only the Donnan exclusion is taken into account.[71, 168, 169, 176–180]

The Donnan exclusion implies the electrostatic exclusion of co-ions with the same sign of charge as that of fixed ions in the membrane.[70, 73] The dielectric exclusion refers both to cations and anions. The ions are excluded from a narrow pore in the membrane, because the presence of an ion in the pore gives rise to a polarization charge of the same sign on the pore surface.[166, 181] The phenomenon is well known in electrostatics,[182] and it is manifested in membrane pores, since the dielectric constant of the membrane matrix is markedly lower than the dielectric constant of the pore solution.[183] Therefore, this phenomenon can be considered as an additional rejection mechanism for any ion, irrespective of the sign of its charge.[166, 181, 184, 185]

The Donnan exclusion, steric hindrance and dielectric exclusion can be taken into account through the following equation:[183]

$$\frac{c_i^{\text{pore}}(x=0)}{c_i(x=0)} = \phi_i \exp(-z_i \Delta\psi_{\text{D}_i^0}) \cdot \exp(-z_i^2 \Delta W_0) \qquad (7)$$

where $c_i^{\text{pore}}(x=0)$ and $c_i(x=0)$ are the concentrations of ion i in the pore solution and in the external solution at the solution/membrane interface (with the coordinate $x=0$), respectively; $\Delta\psi_{\text{D}_i^0}$ and ΔW_0 are the dimensionless Donnan potential difference and the dimensionless ion solvation energy difference, which arise on passing from the external solution to the pore solution at $x=0$; ϕ_i is the partition coefficient taking account of the steric effect,

$$\phi_i = 1-\lambda_i^2 \qquad (8)$$

where $\lambda_i = r_i/r_{\text{pore}}$, r_i is the Stokes radius of the ion, r_{pore} is the pore radius. It can be seen that ϕ_i decreases as the ion radius increases. The exponent including $\Delta\psi_{\text{D}_i^0}$ expresses the Donnan equilibrium and takes into account the electrostatic exclusion of ions; the dielectric exclusion is taken into account through the term ΔW_0, which is expressed as a function of the Debye lengths in the external and pore

solutions, pore radius and the dielectric constants of the solution and the membrane matrix.[183]

Most of recent models are based on representing an NF membrane as a system of pores. The extended Nernst–Planck equation, which includes diffusion, electromigration and convection contributions to the transport of ion i, is used to describe the ion and solvent transport in thin pores $\sim$1 nm (or more) in diameter. Some authors modify this equation to take into account the hindered transport in thin pores the size of which is comparable with the molecular dimensions.[183, 186, 187] Bandini and Vezzani[183] introduced a correction (hindrance) factor $K_i^{\mathrm{d}} < 1$ for the diffusion coefficient of species i in the pore

$$D_i^{\mathrm{pore}} = K_i^{\mathrm{d}} D_i^0 \tag{9}$$

(D_i^0 is the diffusion coefficient of ion i in water at infinite dilution); this takes into account the decrease in the ion i mobility when it moves along a narrow channel. The contribution of convection in the membrane pores, $fK_i^{\mathrm{c}} c_i^{\mathrm{pore}}$, was also calculated using the hindrance factor $K_i^{\mathrm{c}} < 1$. The coefficients K_i^{d} and K_i^{c} are known functions of λ_i (Ref. 183).

The assumption of local electroneutrality[174, 183] and the Poisson equation, taking account of the deviation from electroneutrality,[188, 189] are alternative additional conditions, which are used together with the Nernst–Planck equation to describe the transport both in the external solution and in the pore solution of the membrane. The deviation from electroneutrality is significant for thin barrier layers, since the space charge region has a high resistance to the transport of like-charged divalent ions. However, the use of the Poisson equation complicates the mathematical problem. Yaroshchuk *et al.*[190] developed a simpler approach, according to which the deviation from local electroneutrality in the membrane pores is taken into account *via* the equilibrium concentration profiles of ions in membrane pores in the Poisson–Boltzmann approximation.

Apart from the extended Nerst–Planck equations, modelling can be based on the Kedem–Katchalsky equations,[191] which follow from irreversible thermodynamics.[169, 192] Initially, these equations were formulated in an integral form using transport coefficients averaged over the membrane thickness. Later, Spiegler and Kedem[193] presented a differential form of these equations based on the virtual solution concept (a hypothetical electrically neutral solution at equilibrium with a small membrane volume at point x). These equations involve the so-called practical transport coefficients, which are generally functions of the virtual solution concentration varying along the x coordinate. Determination of the concentration-dependent transport coefficients is a complicated problem.[194] An interesting approximation is based on the Spiegler and Kedem equations using concentration-independent transport coefficients.[174, 195] Filippov and Philippova[196] combined the Kedem–Katchalsky equations with the cell model developed by Happel and Brenner.[197] A cell is a porous charged spherical particle enclosed in a liquid spherical shell. A membrane structure is represented as an ordered set of such elementary cells. This method can be used to model the hydrodynamic permeability,[198] electroosmotic permeability and specific electrical conductivity[199] and to calculate the capillary-osmosis and reverse-osmosis coefficients.[200] Other versions of the cell model can be used to describe the transport parameters of ion-exchange and NF/RO membranes.[201–204]

The Spiegler–Kedem–Katchalsky model is used for theoretical description of various separation processes such as NF membrane-based extraction of heavy metals,[194, 205] water,[206] amino acids,[207] dyes[208] and so on[209, 210] from solutions.

The Kedem–Katchalsky equations are also applied to model ED separation processes. De Jaegher *et al.*[211] used the Kedem–Katchalsky equations to model the evolution of concentration profiles in sodium, chloride and dodecyl sulfate mixed solutions during electrodialysis taking account of membrane fouling.[212]

Femmer *et al.*[213, 214] developed a general model and software called EnPEn for the simulation and quantitative description of ion transport through layer-by-layer membranes. The model is based on the Nernst–Planck–Poisson equation and the conservation laws. This enables simulation of the behaviour of a system comprising n ions, n electrolyte layers and n polyelectrolyte layers. The polyelectrolyte layers form a layer-by-layer membrane usually consisting of a substrate and several active film bilayers. Evdochenko *et al.*[110, 215] utilized this software and the COMSOL Multiphysics software to investigate the effect of charge distribution in the multilayer film on the selective transport of mono- and divalent ions through multilayer NF membranes. It was shown that a multilayer active film on a substrate membrane separates mono- and divalent ions more efficiently if one layer has a clear boundary with the other one; the separation factor decreases when the layers are mixed, that is, one nanosized layer penetrates into the other one.

In the mathematical problem, some authors[174, 183] use the transmembrane volume flux (f) as an independent parameter, while other authors[188, 189] calculate the f value using the Navier–Stokes equation to model the solvent transport in a pore.

Dirir *et al.*[189] proposed a polyelectrolyte multilayer membrane as a bundle of straight cylindrical pores. The authors (like the authors of some other publications, *e.g.*,[188, 216]) applied the so-called homogeneous approximation in which the electric potential distribution in the pore was assumed to be independent of the radial coordinate. It was assumed that the pore radius is much smaller than the Debye length, which characterizwa the electrical double layer at the pore wall. In this case, the homogeneous approximation actually holds and its use markedly simplifies the calculations.

4.2. Mechanistic and data-driven approaches

The above models are sometimes called mechanistic models,[213, 214, 217] or first-principles models.[218] They are based on physicochemical consideration of the processes described using the fundamental Nernst–Planck framework and other fundamental equations.

An alternative approach is the data-driven modelling using neural differential equations. Artificial neural networks have been successfully used in the past decade for tackling various problems such as image recognition and natural language processing. A neural network learns from data rather than from fundamental laws. This approach is used more and more widely in chemical engineering applications, in particular, for membrane separation processes.[219–222] Rall *et al.*[223, 224] used artificial neural networks to predict ion separation by multilayer membranes. The

approach was used to optimize the manufacturing conditions in order to improve the permeability of these membranes. Artificial neural networks have some advantages over the classical mechanistic approach. In particular, this reduces the computation time needed for the design of membrane units for ion separation/recovery.[221] The use of neural networks for the modelling of processes is easier, since there is no need for researchers to thoroughly know the physicochemical laws that govern the system behaviour. A fairly promising approach is to combine mechanistic and data-driven models.[225] In this case, it is possible to take advantage of both approaches: the self-learning ability of artificial neural networks and high predictive power of mechanistic models. As an example of this hybrid modelling, consider studies by De Jaegher *et al.*[217,226] dealing with colloidal fouling of ion-exchange membranes during electrodialysis of natural solutions.

4.3. Modelling of competitive ion transport through ion-exchange membranes during electrodialysis

The main theoretical views on the competitive transport of two different counter-ions (ions 1 and 2) were developed back in the 1970s and 1980s.[227–231] A membrane system is considered as a multilayer assembly, including one (or several) layers of the membrane and two adjacent diffusion layers of the solution. At low current densities (much lower than the limiting current density, $J_{\lim}$), the competitive transfer of counter-ions 1 and 2 is controlled by their transport through the membrane.[228,232,233] The membrane is almost impermeable to co-ions (*e.g.*, Cl^- for the cation-exchange membrane), and at a low current density ($J \to 0$), the fluxes of counter-ions of sort i through the membrane are proportional to the product of the concentration of these ions ($\bar{c}_i$) by their diffusion coefficient ($\bar{D}_i$) in the membrane [73,228]

$$j_i^{J\to 0} = \frac{\bar{D}_i z_i^2 \bar{c}_i}{\sum\limits_{i=1,2} \bar{D}_i z_i^2 \bar{c}_i} \frac{J}{z_i \mathrm{F}} = \frac{T_i J}{z_i \mathrm{F}} \tag{10}$$

As the current increases, the concentration polarization of the membrane is enhanced: concentration gradients of ions in the solution and in the membrane appear and increase. In the membrane, the concentration gradients of counter-ions are arranged in such a way that the diffusion transport, which increases with increasing current, reduces the electromigration of the preferentially transported counter-ions and enhances the electromigration of the rejected counter-ions. The resistance of the solution subjected to desalination increases with increasing current. As a result, the membrane control over the ion fluxes gradually switches to the control by the depleted diffusion layer. As a result, the membrane selectivity to the transport of competing counter-ions decreases. Solution of the Nernst–Planck equation showed that at a relatively large potential drop, the concentrations of both sort 1 and sort 2 ions near the membrane surface tend to zero (the current density approaches its limiting value). In this case, the fluxes of competing ions no longer depend, in the first approximation, on the properties of the membrane, but are determined only by the thickness of the diffusion layer, the diffusion coefficients of the ions in the solution and ion concentrations in the bulk solution [228]

$$j_i^{\lim} = \frac{D_i^0 (1 - z_i/z_a) c_i}{\delta} \tag{11}$$

where z_a is the charge number of co-ions, δ is the diffusion layer thickness; the superscript lim means that the considered state refers to the limiting current, *i.e.*, to the maximum current possible under the electroneutrality condition in the absence of other transport mechanisms except for electrodiffusion. Note that the $j_i^{\lim}$ value depends on the transport of co-ions through the membrane, which in turn depends on the membrane thickness, ion-exchange capacity, the diffusion coefficients of ions in the membrane, and the Donnan constant, determining the co-ion concentration.[234] However, this dependence is rather weak; the increase in $j_i^{\lim}$ above the value set by relation (11) is caused by the current exaltation effect:[235] the flux of counter-ions increases, since the system tends to local electroneutrality. The co-ions that have passed through the membrane and released into the depleted solution near the membrane surface attract counter-ions from the bulk solution to the surface.[236] Although the fluxes of competing ions may increase by several percent due to the exaltation effect, their ratio virtually does not change.

Thus, in the case of competitive transport of two different counter-ions (1 and 2) through a single-layer membrane, the permselectivity coefficient of the membrane varies between $S_{1/2}^{J\to 0}$ (at low currents) and $S_{1/2}^{\lim}$ (when the limiting current is approached) [73]

$$S_{1/2}^{J\to 0} = \frac{\bar{D}_1 z_1^2 \bar{c}_1 c_2}{\bar{D}_2 z_2^2 \bar{c}_2 c_1} \tag{12}$$

$$S_{1/2}^{\lim} = \frac{D_1^0 (1 - z_1/z_a)}{D_2^0 (1 - z_1/z_a)} \tag{13}$$

The dependence of $S_{1/2}$ on the current density (or potential drop) for a single-layer membrane is monotonic. This type of dependence was found in a large number of studies, especially in the 1980s in Japan, where large-scale investigations were carried out for the production of table salt from sea water by electrodialysis. Zabolotsky and Nikonenko [73] summarized these data in one plot containing the results of studies of 17 ion-exchange membranes.

For a long time, it was believed that the formation of a thin modifying layer on the surface of a substrate membrane can increase the permselectivity of the composite membrane, while preserving the monotonic dependence of $S_{1/2}$ on $J/J_{\lim}$, and that the $S_{1/2}$ value at the limiting current density is still determined by the properties of the diffusion layer according to Eqn (13). This course of dependence was confirmed by experimental results (Fig. 11).

However, recently Golubenko and Yaroslavtsev [238] proved experimentally and theoretically that the dependence of $S_{1/2}$ on $J/J_{\lim}$ has an extremum. This type of dependence was also confirmed by Gorobchenko *et al.*,[239,240] who used a mathematical model based on the Nernst–Planck–Poisson equations (Fig. 12).

As follows from their model,[239] at low current densities, the value of $S_{1/2}$ is controlled by the substrate membrane, as in the case of a single-layer membrane, *i.e.*, Eqn (12) approximately holds. As a rule, commercial IEMs (*e.g.*, CMX sulfonate cation-exchange membrane) predominantly transfer divalent ions (ions 2), as they are selectively absorbed by the membrane due to stronger electrostatic attraction to the fixed ions.[70] As the current increases, the concentration of divalent ions 2 near the membrane surface

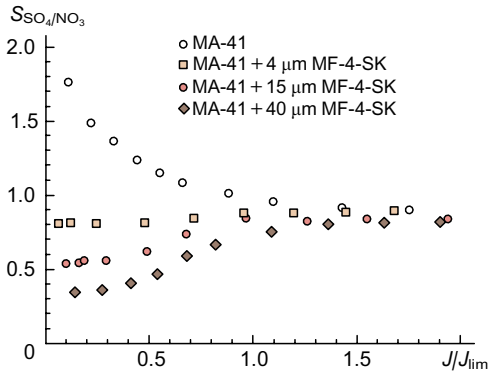

Figure 11. Permselectivity coefficient of MA-41 anion-exchange membrane and modified membranes *vs.* J/J_{lim} ratio in the separation of the SO_4^{2-} and NO_3^- ions. Reprinted from Ref. 237.

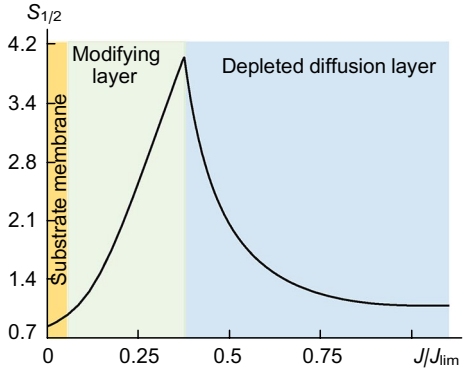

Figure 12. Dependence of the $S_{1/2}$ ratio of a bilayer IEM on J/J_{lim}. The calculation was performed using a one-dimensional model based on the Nernst – Planck – Poisson equations.[239] An increase in the current induces replacement of the rate-determining stage (shown in the plot) of the competitive counter-ion transfer (1 is monovalent ion, 2 is divalent ion); the conventional boundaries of the stages are indicated by different colours. The substrate parameters correspond to the Neosepta CMX cation-exchange membrane; the thickness of the modifying layer is 30 nm; concentration of fixed groups in this layer is 2 mol (L of the membrane)$^{-1}$.

decreases more rapidly than the concentration of monovalent ions 1 (Fig. 13, $J/J_{lim} = 0.3$).

Both competing ions are co-ions for the active modifying layer. The divalent co-ion is more strongly rejected by this layer, and a rapid decrease in the co-ion concentration near the layer surface results in a significant increase in the layer resistance to the transport of ion 2. As a result, the transport starts to be controlled by the modifying layer, which becomes almost impermeable to ions 2, but continues to transfer ions 1. When $J/J_{lim} = 0.7$ (calculation conditions), the concentration of ions 1 near the modifying layer approaches zero, whereas the concentration of ions 2 does not differ much from that in the bulk solution. Simultaneously, the flux of ions 1 approaches its maximum, and the flux of ions 2 can be close to zero; finally, the $S_{1/2}$ value reaches its maximum (Fig. 13, $J/J_{lim} = 0.7$). When the potential drop increases above the value corresponding to the maximum in the $S_{1/2}$ *vs.* J/J_{lim} curve, the increase in the current is provided almost exclusively by ions 2, with the permselectivity towards ions 2 being lost. As the limiting current is approached, the control is taken by the depleted diffusion layer, as in the case of a single-layer membrane; $S_{1/2}$ tends to a value determined by relation (13).

Thus, the presence of a thin modifying layer containing fixed ions with a charge opposite to the substrate membrane charge makes it possible to achieve a high monovalent-ion permselectivity. The higher the charge density of fixed ions in the modifying layer and the greater the modifying layer thickness, the greater the permselectivity of the bilayer membrane. However, as the charge density of the fixed ions and the modifying layer thickness increase, the current density corresponding to the $S_{1/2}$ maximum shifts to lower currents. Here, the trade-off is observed between the selectivity and the permeability of the composite membrane; the same situation was found previously for gas separation[241–244] and other types of membranes:[63, 127, 136, 245] highly selective membranes cannot have high permeability, and, conversely, high permeability of a membrane can be achieved at the expense of its selectivity. In experiments described by Achoh *et al.*,[237] the modifying layer deposited on the surface of the MA-41 membrane is relatively thick (> 4 μm). Apparently, the maximum in the $S_{1,2} - J/J_{lim}$ dependence corresponds to a current that is too low to be used in the experiments. According to the theoretical estimates of Gorobchenko *et al.*, [239] the thickness of the modifying layer bearing an opposite charge should be 20 – 50 nm (when the fixed ion concentration is ~1 mol L^{-1}) for the $S_{1/2}$ maximum to be located near $J = 0.5\,J_{lim}$.

5. Novel promising highly selective methods for lithium recovery

The membrane methods described above are traditionally classified into processes using either a pressure gradient or

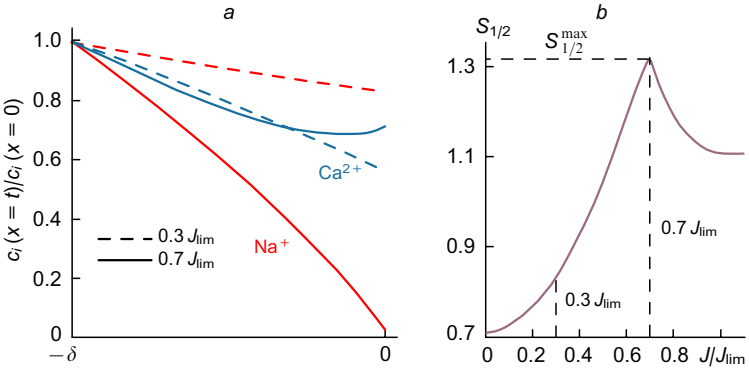

Figure 13. Concentration profiles of Na^+ and Ca^{2+} ions at current densities $J = 0.3\,J_{lim}$ and $J = 0.7\,J_{lim}$ in the depleted diffusion layer that is adjacent to a bilayer membrane with a deposited anion-exchange layer and a cation-exchange substrate layer (*a*); $S_{1/2}$ *vs.* J/J_{lim} for the composite membrane (*b*). The calculation was performed using a one-dimensional model based on the Nernst – Planck – Poisson equations.[239]

an electric potential gradient as the driving force. The use of these methods almost does not require chemical reagents, which is an important advantage over traditional lithium recovery and recycling techniques. However, they do not always provide high selectivity in the extraction of lithium, especially when it comes to Li^+ recovery from a mixture of singly charged cations. This Section contains data on the latest advances in membrane methods for highly selective extraction of lithium using novel approaches other than conventional ED and NF.

5.1. Methods based on ion exchange and diffusion

Zante *et al.*[246] prepared an extraction system (supported liquid membrane) consisting of heptafluorodimethyloctanedione and tri-n-octylphosphine oxide ligands dissolved in dodecane, with permselectivity for lithium over sodium of ~400. However, the lithium ion flux density through this membrane was moderate [$j_{Li^+} = 0.052$ mol $(m^2\ h)^{-1}$]. The separation mechanism is as follows: lithium is extracted from ammonia solution at the feed solution/liquid membrane interface *via* ion exchange to release a proton; then the lithium ion as a part of the lipophilic complex is diffusively transported towards the liquid membrane/receiving phase interface where lithium is released by exchange with the protons of the acid that is present in the receiving compartment from the very beginning. The high selectivity for lithium is attributable to the fact that lithium ion has the highest charge density among alkali metal ions.

Yang *et al.*[247] proposed an electrolysis-based technique for extraction of lithium from seawater and recovery of lithium metal (Fig. 14). As the lithium ion-selective membrane, Nasicon type solid electrolyte was used in this device. The method envisages that the device can be powered by solar energy. Laboratory tests demonstrated that, under optimal conditions, lithium is transferred through the selective membrane at a rate of $\sim 8.5 \times 10^{-3}$ mol $(m^2\ h)^{-1}$ and is deposited on the copper cathode. This device is promising since most of lithium reserves are concentrated in the global ocean water.

Palagonia *et al.*[248] studied a flow-through ion-exchange system, which included a lithium manganese oxide electrode sandwiched between two nickel hexacyanoferrate (NiHCF) electrodes. Under the action of an external electric field, lithium ions are selectively transferred through the lithium manganese oxide electrode. Treatment of 1.35 L of a feed solution containing LiCl (1 mmol L^{-1}) and NaCl (100 mmol L^{-1}) gave 5 mL of LiCl (100 mmol L^{-1}) with 94% purity. According to our estimates, this corresponds to relatively high recovery rate amounting to ~0.9 mol $(m^2\ h)^{-1}$.

A lithium composite membrane with incorporated lithium ion-conducting glass ceramic particles (Fig. 15*a*), proposed by Ounissi *et al.*[147,148] (see also Section 3), was applied more successfully in diffusion dialysis (DD) and cross ionic dialysis (CID)[249] than in electrodialysis. In the case of DD, both counter-ions and co-ions can pass through the IEM to maintain the electroneutrality. In the case of CID, only counter-ions are transferred through the membrane, while co-ion transport is suppressed by the Donnan exclusion. Thus, Li^+ ions (accompanied by chloride ions in the case of DD) diffuse through the membrane owing to the presence of lithium ion-conducting glass ceramics, which gives rise to a selective channel for Li^+ in the anion-exchange polymer (Fig. 15*b*).

Diffusion dialysis of a solution with $c_{Na^+}/c_{Li^+} = 40$ ($c_{tot} = 4.1$ g L^{-1}) for 24 h resulted in extraction of 16.6%

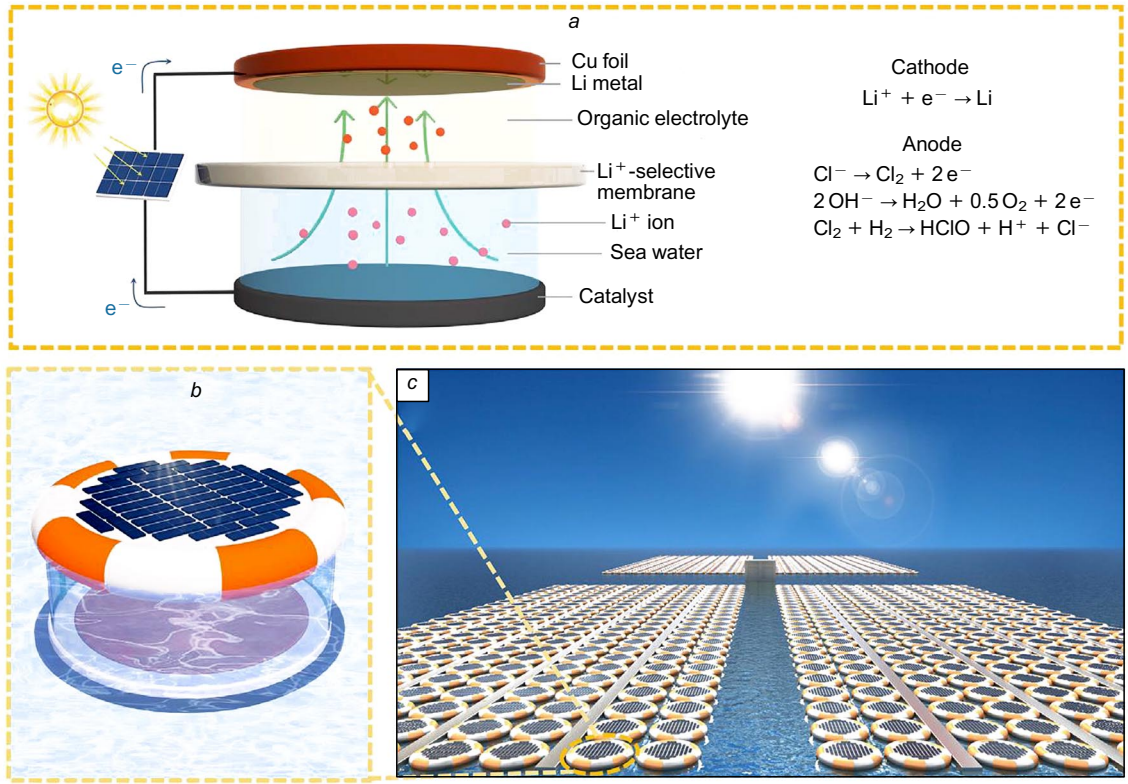

Figure 14. Structure and mechanism of the solar-powered lithium extraction device (*a*); single unit (*b*) and scale-up device array on the sea (*c*).[247] Published with permission from Elsevier.

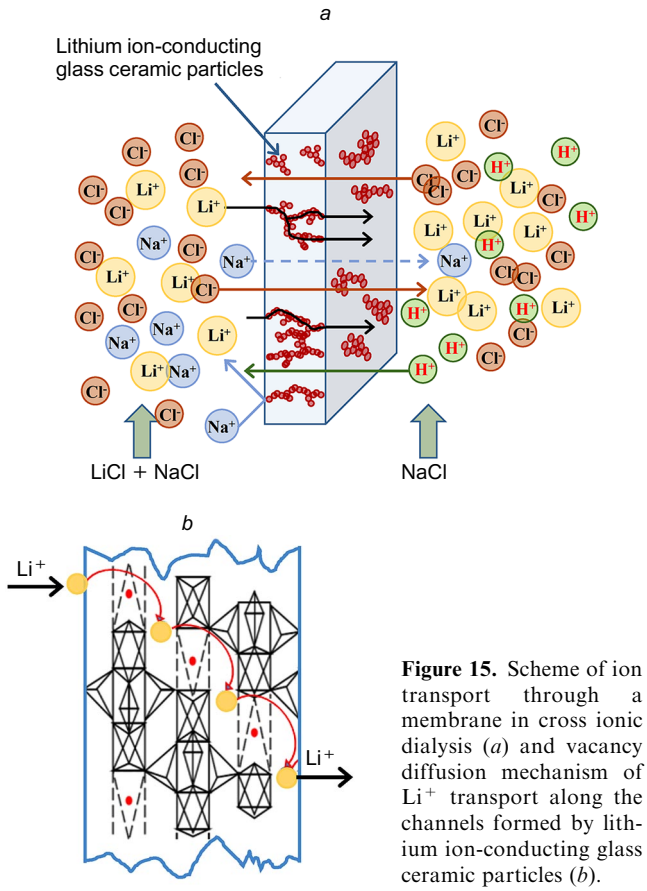

Figure 15. Scheme of ion transport through a membrane in cross ionic dialysis (*a*) and vacancy diffusion mechanism of Li^+ transport along the channels formed by lithium ion-conducting glass ceramic particles (*b*).

of Li^+, with only 0.003% of Na^+ being present in the concentrate; this corresponds to $S_{Li^+/Na^+} = 5500$. In the case of CID, the product contained 36.8% of Li^+ and 0.11% of Na^+, with the S_{Li^+/Na^+} value being 930. Despite the indicated advantages of CID, the ion transfer by this process remains limited and slow [$j_{Li^+} \approx 0.05$ mol $(m^2\ h)^{-1}$]. These limitations can be overcome by stimulating the exchange processes through the membrane by applying a concentration gradient of compensating cations in the case of CID [$j_{Li^+} \approx 0.1$ mol $(m^2\ h)^{-1}$] or an electrical potential gradient in ED [$j_{Li^+} \approx 0.1$ mol $(m^2\ h)^{-1}$]. However, in this case, the selectivity of lithium transfer decreases, which is in line with the known trade-off effect between the membrane permeability and selectivity in separation processes.

Kazemzadeh *et al.*[250] developed and studied a series of polymer inclusion membrane systems containing green polyol as the base polymer, 12-crown-4 (12C4) as the carrier and 1-butyl-3-methylimidazolium chloride ionic liquid. Like in the case of liquid membranes, the selectivity of lithium extraction is provided by complex formation, in particular, lithium forms a nesting complex with 12C4 (with the greatest negative free energy), whereas the other cations form so-called perching complexes. Meanwhile, adjusting the ratio between the ionic liquid and the carrier (1 : 2) and the use of green polyol for cross-linking in the best GZ-PIM3 membrane give rise to an optimal porous structure, which prevented the transfer of multiply charged ions with large hydrated radii. The GZ-PIM3 membrane exhibits the highest selectivity towards lithium ions over Na^+, K^+, Ca^{2+} and Mg^{2+} ions present in the solution in equimolar ratios (according to our calculation, $S_{Li^+/M^{n+}} = 13.2$, 20.3, 196 and 260, respectively); furthermore, the lithium flux is relatively high [$j_{Li^+} \approx 0.63$ mol $(m^2\ h)^{-1}$].

There are known cases of using commercial track-etched membranes (similar to NF membranes in their properties) with narrow pores in electrodialysis. This ensures simultaneously high ion fluxes and high permselectivity due to the sieve effect.[251, 252] Thus, a 2 μm-thick track-etched nanoporous Lumirror® membrane showed a high transfer rate of alkali metal ions [*e.g.*, $j_{Li^+} = 10.8$ mol $(m^2\ h)^{-1}$ in 1 M LiCl], while the transfer rate of ions with a great hydrated radius was low [$j_{Mg^{2+}} = 0.12$ mol $(m^2\ h)^{-1}$ in 1 M $MgCl_2$]. Testing of the membrane in a Li^+ and Mg^{2+} binary mixture (1 : 1) with a total concentration of 1 mol L^{-1} showed that the fluxes of these ions through the membrane sharply decrease [$j_{Li^+} = 0.014$ mol $(m^2\ h)^{-1}$ and $j_{Mg^{2+}} = 6.7 \times 10^{-4}$ mol $(m^2\ h)^{-1}$] under the same experimental conditions.

5.2. Hybrid electrobaromembrane methods

Usually, the external electric field and the pressure field are used separately in membrane systems. These processes are called electrically driven (or electromembrane) and pressure-driven (or baromembrane) processes, respectively. A different approach is employed in hybrid electrobaromembrane methods in which the separation is induced by both driving forces, electrical and mechanical ones. The former is generated by applying a potential difference and the latter is caused by a pressure drop across the membrane.

There are several publications [253, 254, 263, 255–262] in which both driving forces are applied simultaneously for purposes other than the separation of ions. The following major results were obtained in these studies:

— increase in the permeate flux through the membrane due to electroosmotic flow;[255, 256]

— pH change in the compartments between the membrane and the electrodes due to electrode reactions;[256, 257]

— control of solvent and electrolyte fluxes by changing the pressures in the desalination and concentration chambers of the electrodialysis cell;[258–263]

— decrease in the concentration polarization and increase in the fouling resistance.[264–266]

However, processes of this type in which the pressure and electric field gradients act in the same direction can also be used for ion separation.[267, 268] Li *et al.*[268] proposed a selective porous NF membrane (with a mean pore size of ~0.5 nm) consisting of a piperazine copolymer with trimesoyl chloride for the electrodialysis separation of a Li^+/Mg^{2+} mixture. The selectivity mechanism of this membrane is based on the presence of strong electronegative oxygen-containing groups on the membrane surface (Fig. 16 *a*); these groups are polarized by an external electric field and form complexes preferably with Mg^{2+} (Fig. 16 *b*). Under the action of the electric field, Mg^{2+} ions are concentrated at the membrane surface and form a positively charged layer, which prevents further transfer of Mg^{2+} through the membrane (Fig. 16 *c*). The magnesium rejection is almost 100%. Lithium ions have a lower hydration energy and charge number than Mg^{2+}; this accounts for the high selectivity of Li^+ transfer through the membrane under the action of both a pressure field and an electric field [$S_{Li^+/Mg^{2+}} > 5000$, $j_{Li^+} = 0.55$ mol $(m^2\ h)^{-1}$].

Yet another attractive process can be used for the extraction of lithium from solutions, which uses of oppositely directed pressure and electric fields for ion separation

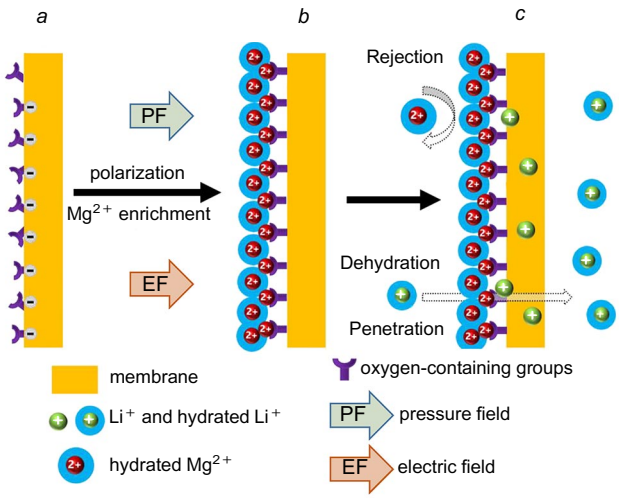

Figure 16. Mechanism of separation of Li^+ and Mg^{2+} ions by a hybrid electrobaromembrane method with co-directional electric and pressure fields. (*a*) NF membrane surface polarized by electric field; (*b*) formation of magnesium complexes with oxygen-containing groups and enrichment of the membrane surface with Mg^{2+} ions; (*c*) rejection of Mg^{2+} ions and permeation of Li^+ ions.[268] Published with permission from Elsevier.

using porous membranes. In this case the separation is due to the difference between ion mobilities in an electric field rather than due to the use of membranes with a selective layer.[74, 269]

This approach was first described back in 1946 by Brewer *et al.*,[270, 271] who separated potassium isotopes (Fig. 17). The separation was performed in a glass tube packed with sand. The K^+ isotopes moved from the right to the left in an electric field, while the solution flowed from the left to the right. The solution flow rate had to be sufficiently high to bring the net transport of the slowest isotope to zero. Under these conditions, the mixture component migrating at the highest rate is concentrated in the left section of the tube, while the slowest component is accumulated in the right section.

This ion separation method, called counter-current electromigration [271] (or counter-current electrophoresis [272]) was widely used in the subsequent years to separate ions,[273, 274] proteins [275] and especially isotopes.[276, 277] More recently, the design of the separation system was changed, particularly, the glass tube filled with sand, glass beads, *etc.* was replaced by a column with compartments separated by diaphragms. This technique makes it possible to fractionate components of the feed solution.[274]

Kontturi and co-workers [278–284] were the first to use a porous membrane and auxiliary ion-exchange membranes instead of diaphragms to isolate the ionic fractions. The narrow pores of microporous membranes such as a Millipore SC ensured a laminar flow of the solution and reduced the deviations of flow velocity from the direction perpendicular to the membrane surface. A relatively thick membrane provided a high separation efficiency in the case of an appropriate choice of the convection velocity and electric current intensity.[282] Additional important advantages of this system were the scalability and potential industrial applicability owing to the convenient design.[285]

The efficiency of this technique was tested in the separation of ions of different mobilities in systems containing strong electrolytes,[278, 279, 285, 286] weak electrolytes [281] and multi-ion mixtures and in removal of trace ions.[280] In the separation of Li^+/Na^+, Li^+/K^+ and Li^+/Ca^{2+} binary mixtures, the $S_{Li^+/M^{n+}}$ ratios were 0.35, 0.085 and 0.27, respectively. This means that ions of competing metals were mainly transported through the membrane [0.28, 0.44 and 0.44 mol $(m^2\ h)^{-1}$, respectively], while lithium remained in the feed solution (the loss was negligible). In the case of processing of a ternary mixture of Li^+, Na^+ and K^+, the separation factor decreased 1.5–2-fold.[280]

Over a long time (approximately since 1990), the number of publications dealing with the counter-current electromigration increased slowly. However, in the last 2–3 years, the interest in this method has ramped up. The reasons are, apparently, both the growing demand for efficient processes for separating various ions (primarily lithium) from mixed solutions and the appearance of membranes that make it possible to solve this task using this method. A considerable step forward in the application of this method was made by Tang *et al.*,[287] who investigated the phenomenon of induced electromigration, which differs from counter-current electromigration only by the fact that electromigration is induced by a field generated by forced fluid flow (streaming

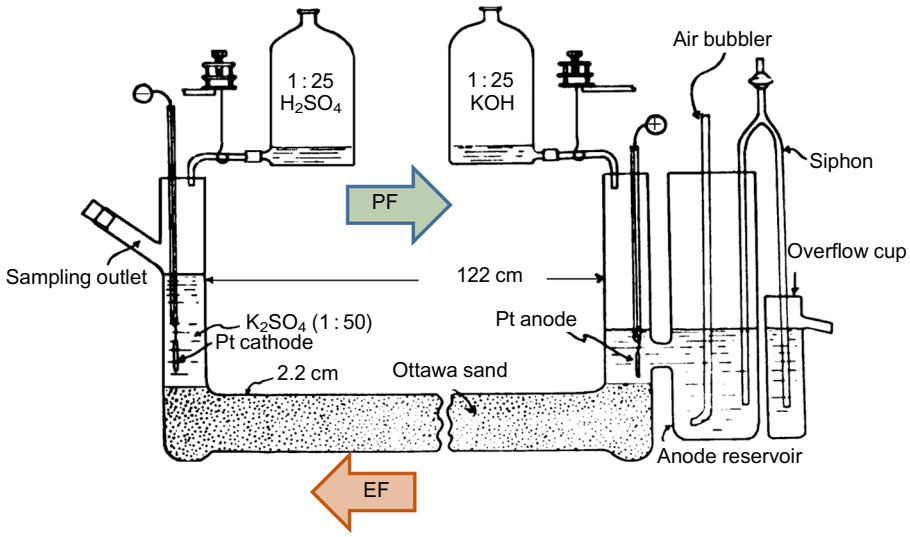

Figure 17. Cell for the separation of potassium isotopes by the counter-current electromigration method.[271] The H_2SO_4, KOH, and K_2SO_4 aqueous solutions were used in the indicated w/w concentrations.

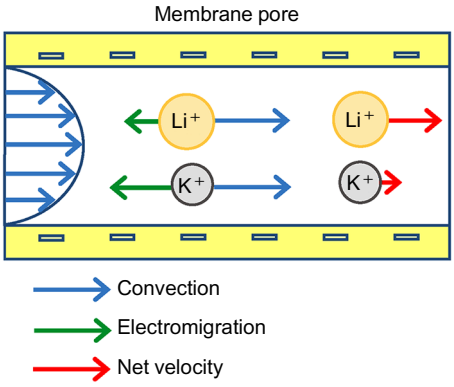

Figure 18. Schematic representation of the velocities of ions separated by induced electromigration within a pore.[287] Electromigration is caused by the appearance of a streaming potential.

potential) rather than by an external electric field (Fig. 18). Experiments on Li^+ and K^+ separation in negatively charged nanopores were carried out. The separation mechanism is as follows: the pressure gradient-induced flow of cations through the membrane pores generates a streaming potential, which initiates the electromigration of cations in the direction opposite to the convective transport direction. A Li^+ ion has a larger hydrated radius than K^+; therefore, the electrophoretic mobility (and, hence, the electrophoretic velocity) of K^+ is almost twice that of Li^+. As a result, K^+ ions are retarded by electromigration to a higher extent than Li^+ ions and move through a negatively charged nanopore at a lower rate than Li^+; the S_{Li^+/K^+} ratio may reach 70.[287]

However, apparently, the induced electromigration method can be effectively applied only for dilute solutions, since an increase in the total solution concentration (ionic strength) results in a decrease in the electric double layer thickness in the pore and in the appearance of co-ions there; this reduces the transport numbers and, hence, the counter-ion fluxes. The use of membranes with narrower pores would lead to undesirable decrease in the counter-ion mobility.

The application of an external electric field the gradient of which is directed opposite to the pressure field gradient (counter-current electromigration) provides a higher performance of the separation process in comparison with induced electromigration (Fig. 19 *a*). The principle of ion separation by counter-current electromigration using a track-etched membrane is illustrated in Fig. 19 *b*.

Yaroshchuk and co-workers[288, 289] conducted Li^+ and K^+ separation experiments in which they set different electric currents at a constant transmembrane pressure drop (ΔP) across a track-etched Sterlitech membrane (USA) in such a way that the K^+ electromigration velocity was greater in magnitude than the convection velocity. At a relatively large ΔP, the resulting K^+ flux approached zero, which ensured efficient separation of Li^+ and K^+ ions. An important feature is that in this case, the less mobile Li^+ ion is transferred from the feed solution through the membrane, which should result in high purity of Li^+ in the receiving solution.

Nikonenko and co-workers[74, 269] also studied the separation of Li^+ and K^+ using a track-etched membrane. The membrane was manufactured at the Joint Institute for Nuclear Research (Dubna, Russia) and conventionally designated as #811. In experiments, the pressure drop

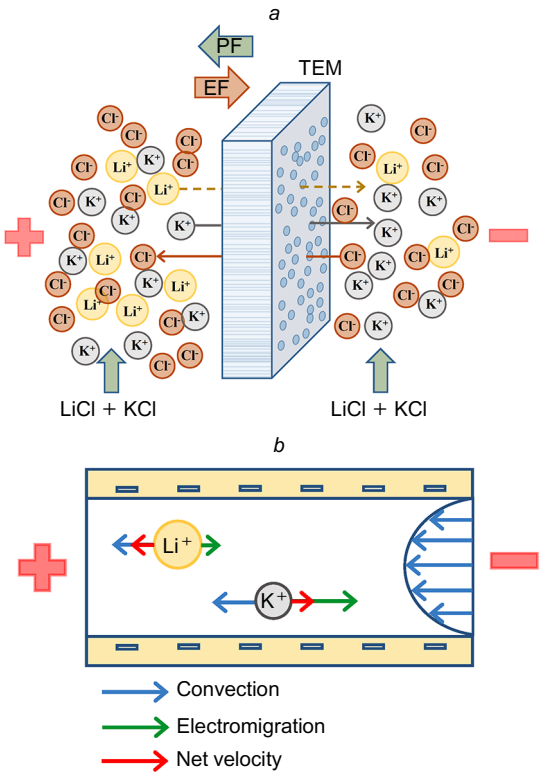

Figure 19. Scheme of Li^+ and K^+ ion separation by counter-current electromigration (*a*) and ion velocities in the pore of a track-etched membrane (*b*). The velocity of electromigration (green arrows) is proportional to the ion mobility; the velocity of convective transfer (blue arrows) is the same for both ions; the net velocities (red arrows) can be directed oppositely.

across the membrane was varied, while the potential drop remained constant (Fig. 20).

When the pressure drop is low, electromigration predominates, while at high ΔP, convection predominates. As ΔP increases, the convective flow reduces the fluxes of both cations. When $\Delta P \approx 0.33$ bar, j_{Li^+} approaches zero, whereas j_{K^+} remains high. A very high permselectivity for K^+ can be obtained under these conditions. When $\Delta P \approx 0.37$ bar, selective Li^+ transport takes place (the flux becomes negative), $j_{K^+} \approx 0$; in the ΔP range between 0.33 and 0.37 bar, the K^+ and Li^+ fluxes have opposite signs.

The obtained dependences that are shown in Fig. 20 imply the presence of three options for the optimized Li^+ and K^+ separation. The first option corresponds to the case where the minimum flux of the less mobile ion (Li^+) is reached in the experiment. In this case, the highest separation rate and the highest K^+/Li^+ permselectivity are achieved (Table 2), with the more mobile cation (K^+) being removed. The second option implies that the fluxes of cations being separated have opposite signs (see Table. 2): it is possible to simultaneously enrich one solution in ion 1 and the other solution in ion 2. In this case, it makes no sense to evaluate the separation selectivity by the S_{K^+/Li^+} or S_{Li^+/K^+} ratio. In fact, the absolute values of the fluxes of both ions are important: the larger the fluxes, the more efficient the separation. It is noteworthy that the case where the fluxes of separated ions move in opposite directions cannot be implemented by other membrane methods.

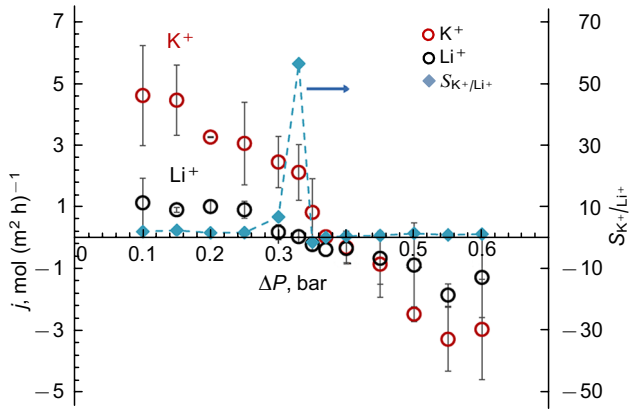

Figure 20. Flux densities of K^+ and Li^+ ions as functions of the applied pressure drop across the track-etched #811 membrane at a constant potential difference of 0.5 V. The dashed line shows the change in S_{K^+/Li^+}. The solution pumped in the left-hand and the right-hand compartments adjacent to TEM is the same: 0.07 M LiCl + 0.13 M KCl. Experimental data were obtained under conditions described in Ref. 74.

Table 2. Comparison of the performances of two processes for Li^+/K^+ separation by counter-current electromigration using polyethylene terephthalate track-etched membranes.[74, 288]

Membrane characteristics	Data of Tang *et al.*[288]	Data of Butylskii *et al.*[288]
Membrane	Sterlitech	#811
Pore diameter, nm	400	35
Pore density, cm^{-2}	2×10^6	5×10^9
Part of the surface occupied by the mouths of the pores, %	0.25	5.5
Feed solution composition	0.05 M Li_2SO_4 + + 0.05 M K_2SO_4	0.07 M LiCl + + 0.13 M KCl
j_{Li^+}, mol $(m^2\ h)^{-1}$	~0.5	~0.02 [a]
		~ −0.23 [b]
		~ −0.4 [c]
j_{K^+}, mol $(m^2\ h)^{-1}$	~0.005	~2.1 [a]
		~0.81 [b]
		~0.015 [c]
S_{Li^+/K^+}	100	59 [c]
S_{K^+/Li^+}		55 [a]
J, A m^{-2}	1500	170
Voltage across the track-etched membrane, V	13	0.5
Energy consumption, kW h $(mol\ Li^+)^{-1}$	15	0.5

Note. Separation options (see the text): [a] first option, [b] second option, [c] third option.

The third option, described also by Yaroshchuk and co-workers,[288, 289] occurs if the minimum flux of the more mobile ion (K^+) is attained; then the less mobile ion (Li^+) is selectively transported through the membrane.[269] In this case, it is possible to recover the more valuable ion (Li^+) from the mixture with a permselectivity coefficient close to that obtained in the first case. However, the flux density of the extracted ion (Li^+) would be lower than the flux density of K^+ extracted using the first option (see Fig. 20 and Table 2).

According to the published data, the ion separation coefficient and the flux density of the exctracted ion, obtained in the counter-current electromigration process and reported by different authors, are rather close. Thus, the S_{Li^+/K^+} ratio varies from 59 (Ref. 74) to 150;[288, 289] the S_{Li^+/Na^+} ratio is somewhat lower and reaches 30.[288] However, the estimates of energy consumption made by Nikonenko and co-workers [74, 288, 289] and Yaroshchuk and co-workers [288, 289] are considerably different (see Table 2), which is attributable to differences in membrane characteristics. In both cases, track-etched membranes made of polyethylene terephthalate were used. As mentioned above, the selectivities and ion fluxes did not differ much; however, the energy consumption was ~30 times lower for the #811 membrane. This result is due to the following causes. First, the pore diameter of the Sterlitech membrane is more than 10 times greater than the pore diameter of the #811 membrane. This results in a low current efficiency: to achieve comparable fluxes, the current density in the case of the Sterlitech membrane is almost 10 times higher than that for the #811 membrane. The transport number of Cl^- ions in the #811 membrane in contact with 0.02 M NaCl is estimated to be approximately 0.1;[290] then the sum of the transport numbers of Li^+ and K^+ in the pores of the #811 membrane is close to 0.9. Second, the part of the membrane surface occupied by pores is approximately 20 times smaller for Sterlitech than for the #811 membrane; this dictates high resistance of the former membrane and the need to apply high voltage (13 V *versus* 0.5 V for #811).

It is also worthy of note that in both electro- and baromembrane processes, the intense selective transport of counter-ions, accompanied by the rejection of co-ions, is associated with the appearance of significant concentration gradients (concentration polarization). In the case of the electrobaromembrane method with oppositely directed electromigration and convection fluxes, the concentration polarization is much lower, since the rejection of co-ions is not significant, while convection makes a larger contribution. This is both a benefit (low energy consumption) and a drawback of the method. The drawback is that it seems to be impossible to simultaneously separate the competing ions and concentrate the solution enriched in the target ion. Nevertheless, the described hybrid electrobaromembrane methods can replace, for example, chemical precipitation stages in the selective separation of lithium from other singly charged cations, which reduces the burden on the environment.

6. Prospects of application of membrane methods

All of the above ion separation methods have their benefits and one common limitation, namely, an increase in membrane permselectivity upon modification is inevitably accompanied by an increase in the membrane resistance. As a consequence, a lower flux of the selectively transferred component is attained at the same driving force (the selectivity/permeability trade-off).[63, 127, 291] The authors of many studies have found that high fluxes and high selectivities can be achieved simultaneously only for separation of H^+ from metal ions.[127] For Li^+/Mg^{2+}, Li^+/K^+, K^+/Mg^{2+}, Na^+/Mg^{2+} and other similar pairs, the trade-off principle holds.[106, 109, 127, 128, 267]

In order to highlight the most promising methods for ion separation, we summarized the achievements of various authors in this field. The data are plotted as j_{cat^+} *vs.* $S_{1/2}$,

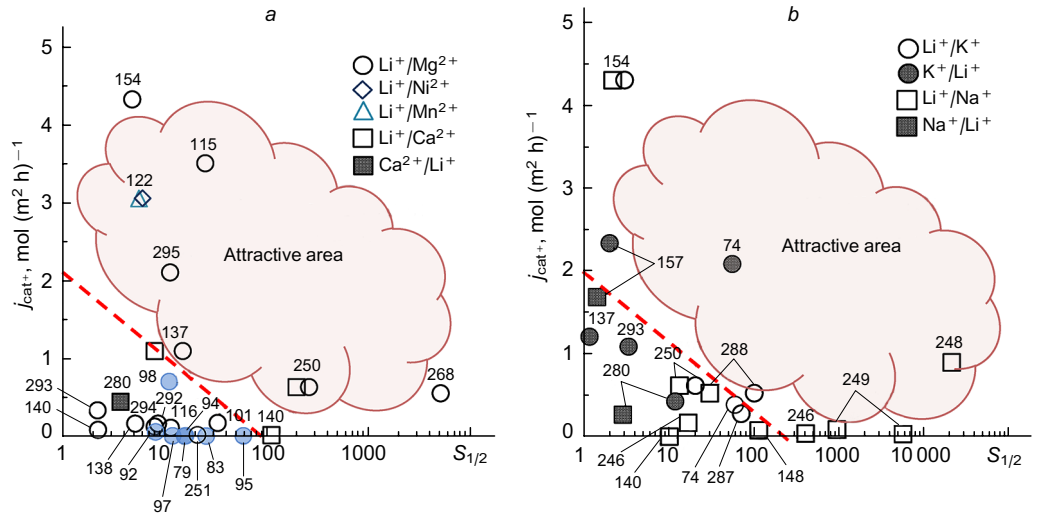

Figure 21. Trade-off diagrams showing the best results in the cation separation: (*a*) separation of monovalent and divalent cations; (*b*) separation of monovalent cations from each other. Blue circles are the results of Li^+/Mg^{2+} separation by nanofiltration (see Table 1); the results of electro- and electrobaromembrane systems were taken from Table 3 The numerals in the drawing are the numbers of original siurces in the list of references.

Table 3. Performance of electromembrane and hybrid electrobaromembrane processes in the selective extraction of Li^+ from various solutions.

Membrane	j_{Li^+}, mol (m² h)$^{-1}$	$j_{M^{n+}}$, mol (m² h)$^{-1}$	Competing cation	$S_{Li^+/M^{n+}}$	Feed solution composition			Ref.
					$c_{M^{n+}}/c_{Li^+}$ (see [a])	c_{Li^+}, g L^{-1}	$c_{M^{n+}}$, g L^{-1}	
Commercial monovalent-ion selective ion-exchange membranes								
Selemion CSO	0.17	0.22	Mg^{2+}	33	150	0.15	22.5	101
	3.5	0.4	Mg^{2+}	25	9.85	8.0	78.7	115
Neosepta CIMS	0.16	0.32	Mg^{2+}	8.6	60	0.14	8.4	292
	0.16	1.2	Na^+	0.88	22	0.14	3.04	292
	0.108	0.16	Mg^{2+}	11.5	60	0.26	15.7	116
	3.05	0.195	Co^{2+}	5.6	3	2.6	7.9	122
	3.05	0.184	Ni^{2+}	6.1	3	2.6	8.0	122
	3.05	0.119	Mn^{2+}	5.4	1.7	2.6	4.4	122
Astom CMB	1.25	2.35	K^+	0.5	5.6	5.46	30.8	157
	1.25	1.7	Na^+	0.7	3.3	5.46	18.1	157
Composite and multilayer cation-exchange membranes and processes based on ion exchange and diffusion								
aCEM/$LiCo_{0.5}Mn_{1.5}O_4$	8.96	0.28	Na^+	0.95	0.1	13.9	1.35	139
CEM-5.5	1.09	0.12	Mg^{2+}	15	3.5	0.35	1.2	137
	1.09	0.28	Ca^{2+}	8	5.8	0.35	2	137
	1.09	1.22	K^+	0.86	5.6	0.35	1.96	137
Sandwiched liquid-	0.079	0.035	Mg^{2+}	2.2	50	1	50	140
membrane	0.013	1.2×10^{-4}	Ca^{2+}	111	5.8	6.94	40.1	140
	0.013	1.3×10^{-3}	Na^+	10	3.3	6.94	23	140
Lithium composite membrane	0.087	2.35×10^{-3}	Na^+	112	10	0.2	2	148
NC-4	4.32	0.25	Mg^{2+}	4.8	1	0.5	0.5	154
	4.32	0.25	K^+	3	1	0.5	0.5	154
	4.32	0.6	Na^+	2.2	1	0.5	0.5	154
M-co-0.50	0.33	1.1	K^+	0.3	5.6	0.35	1.96	293
	0.33	0.15	Mg^{2+}	2.2	3.5	0.35	1.2	293
P-COOH-QSQ	0.16	0.032	Mg^{2+}	5.2	0.3	–	–	138
ZIM QAIPA-20	0.12	0.015	Mg^{2+}	8	0.3	–	–	294
PVDF/liquid membrane	0.052	1.3×10^{-4}	Na^+	400	3.3	0.052	0.17	246
	0.18	1.08	Na^+	16.7	330	6.9×10^{-3}	2.3	246
Ion exchange in a flow-through electrode cell	0.91	0.044	Na^+	20680	3300	6.9×10^{-3}	23	248
Lithium composite	0.045	9.7×10^{-5}	Na^+	5543	40	0.1	4	249
membrane	0.098	1.3×10^{-3}	Na^+	931	40	0.1	4	249

Table 3 (continued).

Membrane	j_{Li^+}, mol $(m^2\,h)^{-1}$	$j_{M^{n+}}$, mol $(m^2\,h)^{-1}$	Competing cation	$S_{Li^+/M^{n+}}$	Feed solution composition			Ref.
					$c_{M^{n+}}/c_{Li^+}$ (see [a])	c_{Li^+}, g L^{-1}	$c_{M^{n+}}$, g L^{-1}	
Nanofiltration membranes								
ENF-Q3	2.1	0.185	Mg^{2+}	11.3	3.5	0.7	2.4	295
GZ-PIM3	0.63	0.048	Na^+	13.2	3.3	0.7	2.3	250
	0.63	0.031	K^+	20.3	5.6	0.7	3.9	250
	0.63	3.2×10^{-3}	Ca^{2+}	196	5.75	0.7	4	250
	0.63	2.4×10^{-3}	Mg^{2+}	260	3.5	0.7	2.4	250
Lumirror®	0.014	6.7×10^{-4}	Mg^{2+}	21	3.5	3.5	12.1	251
NF4	0.55	3.1×10^{-5}	Mg^{2+}	5050	20	0.095	1.9	268
Millipore SC	0.094	0.28	Na^+	0.35	3.3	0.35	0.115	280
	0.031	0.44	K^+	0.085	5.6	0.35	0.195	280
	0.125	0.44	Ca^{2+}	0.27	5.7	0.35	0.2	280
Sterlitech	0.29	4.0×10^{-3}	K^+	70	5.7	0.7	4	287
	0.54	5.4×10^{-3}	K^+	100	5.6	0.35	1.96	288
	0.54	0.018	Na^+	30	3.3	0.35	1.15	288
Sterlitech	—	—	K^+	150	5.6	0.35	1.96	289
#811	0.02	2.1	K^+	0.028	10.5	0.49	5.1	74
	−0.4	0.015	K^+	59	10.5	0.49	5.1	74

[a] Mass ratio.

where j_{cat^+} is the flux density of the target cation (Fig. 21). The trade-off between the membrane permeability evaluated from j_{cat^+} and the separation efficiency evaluated from $S_{1/2}$ can be clearly seen in the diagrams. More detailed data for analysis are presented in Tables 1 and 3. However, it should be mentioned that the parameters of selective separation were evaluated under different experimental conditions and under different driving forces (electric field, concentration gradient, pressure gradient and other). In view of the fact that literature data for membranes have not been obtained under identical experimental conditions, only the best characteristics reported for each membrane were included in the diagrams.

The use of porous NF membranes in the pressure-driven processes enables highly selective extraction of lithium from its mixture with magnesium (see Fig. 21 *a*). However, in these processes water is mainly transported through the membrane, while ions are rejected; hence, lithium ion transfer rate is lower than that in electromembrane processes. Surface modifications of NF membranes is aimed at enhancing the rejection of multivalent ions; meanwhile, monovalent ions are also rejected, although to a lesser extent.

The use of commercial monovalent-ion permselective IEMs makes it possible to attain permselectivity coefficients comparable to those observed for NF membranes; however, the flux of lithium ions is significantly higher for cation-exchange membranes than for NF membrane. For example, the lithium flux through a Selemion CSO membrane exceeds that through the NF membrane by 4–5 orders of magnitude.[115] Special-grade commercial IEMs enable selective extraction of lithium not only from primary sources, but also from secondary sources, which include leach solutions obtained from spent batteries.[122] Meanwhile, new modified IEMs and modified porous NF membranes make it possible to achieve very high separation factors in electrically driven processes.[250, 268] These results are above the upper bounds of trade-off diagrams for monovalent-ion permselective separation and occur in the attractive area (see Fig. 21 *a*).

A more challenging stage in the extraction of lithium is its separation from K^+ and Na^+ ions. This problem is being addressed by many research groups. In practice, chemical precipitation with Na_2CO_3, which is added to a lithium-containing solution in a 1.5–2-fold excess, is used most often.

The achievements of membrane methods (including electromembrane and electrobaromembrane processes and some methods based on ion exchange and diffusion) in the separation of monovalent cations are depicted in Fig. 21 *b*. The upper bound for isolation of a monovalent ion from a mixture of such ions is located approximately at the same level as that for separation of monovalent ions from multivalent ions (see Fig. 21 *a*). As for the separation of monovalent ions from multivalent ions, there is also a trade-off between the membrane permeability and permselectivity. It must be mentioned that there are few cases of relatively high fluxes of lithium (or other component removed from the mixture with lithium) and high separation selectivity that fall into the attractive area in the trade-off diagram. Only the reactor with lithium manganese oxide electrode[248] and the hybrid electrobaromembrane method[74, 288] described above (see Section 5) fit within the conventional boundaries of the attractive area. However the reactor with lithium manganese oxide electrode[248] is suitable for processing of only small volumes of solutions; furthermore, it requires design improvements for withdrawal of the lithium product. In the case of the hybrid electrobaromembrane method, there are also certain limitations. Since track-etched membranes have relatively large pores (average pore diameters of 35 and 400 nm, see Table 2), they are not sufficiently selective to counter-ions (such as Li^+). This leads to a decrease in the energy efficiency of the transfer of Li^+ or competing cations and precludes the simultaneous separation and concentration of target ions, as in the case of electrodialysis.

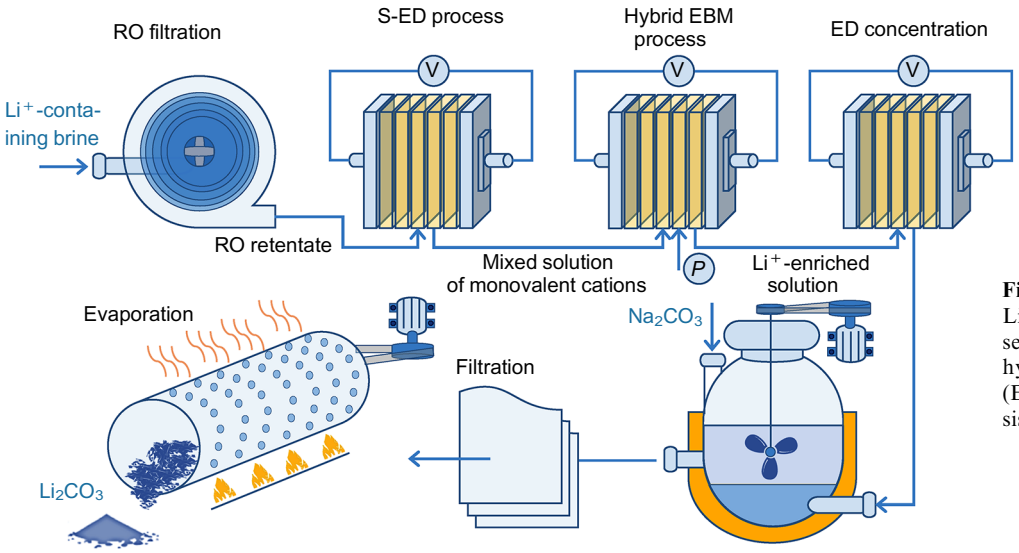

Figure 22. Flow diagram of Li_2CO_3 production process using selective-electrodialysis (S-ED), hybrid electrobaromembrane (EBM) method and electrodialysis (ED) concentration.

Nevertheless, the hybrid electrobaromembrane method may replace the stage of lithium separation by precipitation and reduce its resource intensity. The solutions of individual ions can be concentrated *via* an additional electrodialysis stage. A possible flow diagram for separating and concentrating lithium from a natural or industrial lithium-containing solution using various membrane methods is shown in Fig. 22.

In this process, a lithium-containing natural or industrial brine can be preconcentrated using reverse osmosis (see Section 3.4.2). The RO retentate is then used as a feed solution for the S-ED treatment to separate monovalent ions from multivalent ones. The hybrid electrobaromembrane method serves to extract lithium from a mixture of monovalent cations, while an ED apparatus concentrates the solution in which Li^+ is the predominant component. The preparation of a relatively pure solid Li_2CO_3 salt may require a precipitation stage followed by filtration and evaporation (see Section 2).

7. Conclusion

The rapid growth of lithium consumption and the trend towards an increase in demand for lithium stimulate the scientific development of new methods for recovery of this metal from natural and industrial solutions. The existing traditional reagent-based methods for lithium production are not satisfactory, first of all, regarding their environmental unfriendliness. Currently, this problem is a focus of attention of quite a few laboratories and researchers in various countries. The membrane techniques for lithium extraction are under research and development, but are not used in industry as yet. New membranes and new ways of using them in combination with an external electric field and/or pressure field to form the driving force of the separation process have been proposed. Analysis of the available experimental data suggests that electromembrane methods of lithium extraction are currently more preferable than pressure-driven methods. Of great interest are electrobaromembrane processes in which an electric field and a pressure field are simultaneously applied to the membrane, which makes it possible to separate liquid mixtures of various monovalent ions.

The authors thank Professor P.Yu.Apel for constant assistance in conducting research on track-etched membranes.

This review was supported by the Russian Science Foundation (Project No. 19-19-00381); https://rscf.ru/en/project/19-19-00381/

8. List of abbreviations and symbols

The following abbreviations and symbols are used in the review:

ANN — artificial neural networks,
CID — cross ionic dialysis
DD — diffusion dialysis,
ED — electrodialysis,
EDBM — electrodialysis with bipolar membranes
EF — electric field,
IEM — ion-exchange membrane,
LbL — layer-by-layer;
LIB — lithium ion battery,
MWCNT — multi-walled carbon nanotube,
NF — nanofiltration,
PEI — polyethyleneimine,
PF — pressure field,
RO — reverse osmosis,
S-ED — selective electrodialysis,
TEM — track-etched membrane,
c_i — concentration of ions i in the solution,
$\bar{c}_i$ — concentration of ions i in the membrane,
c_i^{f} — concentration of ions i in the feed solution,
Δc_i^{f} — change in the concentration of ions i in the feed solution,
c_i^{p} — concentration of ions i in the permeate (for NF) or in the concentrate compartment (for ED),
Δc_i^{p} — change in the concentration of ions i in the permeate (for NF) or in the concentrate compartment (for ED),
c_i^{pore} — concentrations of ions i in the pore solution,
c_{tot} — salinity,
D_i^0 — infinite-dilution diffusion coefficients of ions i in aqueous solution,
$\bar{D}_i$ — diffusion coefficients of ions i in the membrane,
D_i^{pore} — diffusion coefficients of ions i in the pore,
f — volume flux,

F — Faraday constant,
J — electric current density,
J_{lim} — limiting current density,
j_{cat^+} — flux density of cations,
j_i — flux density of ions i,
$j_i^{J\to 0}$ — flux density of ions i through the membrane at low electric currents (much lower than the limiting current) in an electromembrane system,
j_i^{lim} — flux density of ions i through the membrane as the limiting current in the electromembrane system has been reached,
K_i^{c} — correction factor for calculating the contribution of convective transport of ions i through the pores,
K_i^{d} — correction factor for calculating the mobility of ions i in membrane pores,
P_i — membrane permeability coefficients for ions i,
ΔP — pressure drop,
r_i — Stokes radius,
r_{pore} — pore radius,
R_i — salt rejection,
s — effective membrane surface area,
$S_{1/2}$ — permselectivity coefficient of the membrane (or separation factor) for competitive transport of two counter-ions (1 and 2),
$S_{1/2}^{J\to 0}$ — permselectivity coefficient of the membrane (or separation factor) for competitive transport of two counter-ions (1 and 2) at low currents,
$S_{1/2}^{\text{lim}}$ — permselectivity coefficient of the membrane (or separation factor) for competitive transport of two counter-ions (1 and 2) for currents approaching the limiting value,
t — time of an experiment,
T_i — integral (or effective) transport number of ions i in the membrane,
V — volume of the feed or permeate (concentrate) solution,
ΔW_0 — dimensionless ion solvation energy difference,
z_{a} — charge number of co-ions,
z_i — charge number of ions i,
δ — diffusion layer thickness,
ϕ_i — partition coefficient taking account of the steric effect,
$\Delta\psi_{D_i^0}$ — dimensionless Donnan potential difference.

9. References

1. M.F.Lagadec, R.Zahn, V.Wood. *Nat. Energy*, **4**, 16 (2019); https://doi.org/10.1038/s41560-018-0295-9
2. C.Grosjean, P.H.Miranda, M.Perrin, P.Poggi. *Renew. Sustain. Energy Rev.*, **16**, 1735 (2012); https://doi.org/10.1016/j.rser.2011.11.023
3. A.Anlauf. *Fairn. Just. Nat. Res. Polit.*, 176 (2016); https://library.oapen.org/bitstream/handle/20.500.12657/46735/oa-9781317269885.pdf?sequence=1#page=177
4. P.Friedlingstein, M.W.Jones, M.O Sullivan, R.M.Andrew, J.Hauck, G.P.Peters, W.Peters, J.Pongratz, S.Sitch, C.LeQuéré, D.C.E. Bakker, J.G.Canadell, P.Ciais, R.B.Jackson, P.Anthoni, L.Barbero, A.Bastos, V.Bastrikov, M.Becker, L.Bopp, E.Buitenhuis, N.Chandra, F.Chevallier, L.P.Chini, K.I.Currie, R.A.Feely, M.Gehlen, D.Gilfillan, T.Gkritzalis, D.S.Goll, N.Gruber, S.Gutekunst, I.Harris, V.Haverd, R.A.Houghton, G.Hurtt, T.Ilyina, A.K.Jain, E.Joetzjer, J.O.Kaplan, E.Kato, K.KleinGoldewijk, J.I.Korsbakken, P.Landschützer, S.K.Lauvset, N.Lefèvre, A.Lenton, S.Lienert, D.Lombardozzi, G.Marland, P.C.McGuire, J.R.Melton, N.Metzl, D.R.Munro, J.E.M.S.Nabel, S.-I.Nakaoka, C.Neill, A.M.Omar, T.Ono, A.Peregon, D.Pierrot, B.Poulter, G.Rehder, L.Resplandy, E.Robertson, C.Rödenbeck, R.Séférian, J.Schwinger, N.Smith, P.P.Tans, H.Tian, B.Tilbrook, F.N.Tubiello, G.R.vanderWerf, A.J.Wiltshire, S.Zaehle. *Earth Syst. Sci. Data*, **11**, 1783 (2019); https://doi.org/10.5194/essd-11-1783-2019
5. A.R.Quinteros-Condoretty, S.R.Golroudbary, L.Albareda, B.Barbiellini, A.Soyer. *Proc. CIRP*, **100**, 73 (2021); https://doi.org/10.1016/j.procir.2021.05.012
6. A.A.Makarov, T.A.Mitrova, V.A.Kulagin. In *Global and Russian Energy Outlook 2019*. (Moscow: ERI RAS — Moscow School of Management SKOLKOVO, 2019). P. 210; https://www.eriras.ru/data/994/rus
7. S.P.Filippov, A.B.Yaroslavtsev. *Russ. Chem. Rev.*, **90**, 627 (2021); https://doi.org/10.1070/RCR5014
8. J.F.Song, L.D.Nghiem, X.-M.Li, T.He. *Environ. Sci. Water Res. Technol.*, **3**, 593 (2017); https://doi.org/10.1039/C7EW00020K
9. P.W.Gruber, P.A.Medina, G.A.Keoleian, S.E.Kesler, M.P.Everson, T.J.Wallington. *J. Ind. Ecol.*, **15**, 760 (2011); https://doi.org/10.1111/j.1530-9290.2011.00359.x
10. D.E.Garrett. *Handbook of Lithium and Natural Calcium Chloride*. (The Nederlands: Elsevier, 2004); https://doi.org/10.1016/B978-0-12-276152-2.X5035-X
11. F.Meng, J.McNeice, S.S.Zadeh, A.Ghahreman. *Miner. Process. Extr. Metall. Rev.*, **42**, 123 (2021); https://doi.org/10.1080/08827508.2019.1668387
12. J.Rioyo, S.Tuset, R.Grau. *Miner. Process. Extr. Metall. Rev.*, **43**, 97 (2022); https://doi.org/10.1080/08827508.2020.1798234
13. C.Dessemond, F.Lajoie-Leroux, G.Soucy, N.Laroche, J.-F.Magnan. *Minerals*, **9**, 334 (2019); https://doi.org/10.3390/min9060334
14. P.Christmann, E.Gloaguen, J.-F.Labbé, J.Melleton, P.Piantone. In *Lithium Process Chemistry*. (The Nederlands: Elsevier, 2015). P. 40; https://doi.org/10.1016/B978-0-12-801417-2.00001-3
15. U.S.Geological Survey. In *Mineral Commodity Summaries*. (Natl. Miner. Inf. Cent., USA, 2022); https://doi.org/10.3133/mcs2022
16. Cypress Development Corp. In *Clayton Valley Lithium Project*. (Nevada, USA, 2022); https://www.centurylithium.com/projects/nevada/clayton-valley-lithium-project-nevada/
17. Y.Zhang, Y.Hu, L.Wang, W.Sun. *Miner. Eng.*, **139**, 105868 (2019); https://doi.org/10.1016/j.mineng.2019.105868
18. A.H.Hamzaoui, A.M'nif, H.Hammi, R.Rokbani. *Desalination*, **158**, 221 (2003); https://doi.org/10.1016/S0011-9164(03)00455-7
19. F.Heredia, A.L.Martinez, V.SurracoUrtubey. *J. Energy Nat. Resour. Law*, **38**, 213 (2020); https://doi.org/10.1080/02646811.2020.1784565
20. S.Zavahir, T.Elmakki, M.Gulied, Z.Ahmad, L.Al-Sulaiti, H.K.Shon, Y.Chen, H.Park, B.Batchelor, D.S.Han. *Desalination*, **500**, 114883 (2021); https://doi.org/10.1016/j.desal.2020.114883
21. A.Siekierka, M.Bryjak, A.Razmjou, W.Kujawski, A.N.Nikoloski, L.F.Dumée. *Membranes*, **12**, 343 (2022); https://doi.org/10.3390/membranes12030343
22. B.Swain. *Sep. Purif. Technol.*, **172**, 388 (2017); https://doi.org/10.1016/j.seppur.2016.08.031
23. C.B.Tabelin, J.Dallas, S.Casanova, T.Pelech, G.Bournival, S.Saydam, I.Canbulat. *Miner. Eng.*, **163**, 106743 (2021); https://doi.org/10.1016/j.mineng.2020.106743
24. S.H.Park, J.H.Kim, S.J.Moon, J.T.Jung, H.H.Wang, A.Ali, C.A.Quist-Jensen, F.Macedonio, E.Drioli, Y.M.Lee. *J. Membr. Sci.*, **598**, 117683 (2020); https://doi.org/10.1016/j.memsci.2019.117683
25. N.N.R.Ahmad, W.L.Ang, Y.H.Teow, A.W.Mohammad, N.Hilal. *J. Water Process Eng.*, **45**, 102478 (2022); https://doi.org/10.1016/j.jwpe.2021.102478

26. T.Zhang, W.Zheng, Q.Wang, Z.Wu, Z.Wang. *Desalination*, **546**, 116205 (2023); https://doi.org/10.1016/j.desal.2022.116205
27. Y.Sun, Q.Wang, Y.Wang, R.Yun, X.Xiang. *Sep. Purif. Technol.*, **256**, 117807 (2021); https://doi.org/10.1016/j.seppur.2020.117807
28. X.Li, Y.Mo, W.Qing, S.Shao, C.Y.Tang, J.Li. *J. Membr. Sci.*, **591**, 117317 (2019); https://doi.org/10.1016/j.memsci.2019.117317
29. D.Bradley, L.Munk, H.Jochens, S.Hynek, K.Labay. *US Dep. Inter. US Geol. Surv.*, 1 (2013); https://pubs.usgs.gov/of/2013/1006/OF13-1006.pdf
30. H.Guo, G.Kuang, H.Wang, H.Yu, X.Zhao. *Minerals*, **7**, 205 (2017); https://doi.org/10.3390/min7110205
31. N.K.Salakjani, P.Singh, A.N.Nikoloski. *Miner. Process. Extr. Metall. Rev.*, **42**, 268 (2021); https://doi.org/10.1080/08827508.2019.1700984
32. W.-S.Chen, C.-H.Lee, H.-J.Ho. *Appl. Sci.*, **8**, 2252 (2018); https://doi.org/10.3390/app8112252
33. W.Wang, W.Chen, H.Liu. *Hydrometallurgy*, **185**, 88 (2019); https://doi.org/10.1016/j.hydromet.2019.02.013
34. A.Karrech, M.R.Azadi, M.Elchalakani, M.A.Shahin, A.C.Seibi. *Miner. Eng.*, **145**, 106085 (2020); https://doi.org/10.1016/j.mineng.2019.106085
35. N.Linneen, R.Bhave, D.Woerner. *Sep. Purif. Technol.*, **214**, 168 (2019); https://doi.org/10.1016/j.seppur.2018.05.020
36. T.Tran, V.T.Luong. In *Lithium Process Chemistry*. (The Nederlands: Elsevier, 2004). P. 81; https://doi.org/10.1016/B978-0-12-801417-2.00003-7
37. B.C.Peek. In *NI 43-101 Technical Report*. (Clayton Valley, Nevada, USA, 2021). P. 78; https://noramlithiumcorp.com/site/assets/files/3886/2021-09-21-ni-43-101-report.pdf
38. J.J.Riordan, A.D.Thompson, E.V.Coetzee, S.Nupen. In *NI 43-101 Technical Report*. (DRA Pacific, Australia, 2020). P. 228; https://minedocs.com/20/Falchani_PEA_03192020.pdf
39. C.Pelletier, S.Boudreau, F.Baril, W.R.McBride, E.Poirier, O.Joyal. In *NI 43-101 Technical Report*. (WSP, Canada, 2022). P. 438; https://www.cecorp.ca/wp-content/uploads/161-14192-03_RPT-01_R1_V1_CELC_Rose-FS-2022.pdf
40. H.Samari, R.Moritz, J.T.Harvey, T.Lane. In *NI 43-101 Technical Report*. (Nye County, USA), 2021. P. 208; https://nvlithium.com/wp-content/uploads/2021/10/Bonnie-Claire-PEA-Technical-Report-Final.pdf
41. I.Ezama, C.R.Hoyos, P.Cortegoso,T.Braun. *Tailings and Mine Waste Conference*, 8 (2018); https://dxi97tvbmhbca.cloudfront.net/upload/user/image/Ezama-Hoyos-Cortegoso-Braun-Spent_Brine_Disposal-TMW_Paper20191128190251287.pdf (access date 07.04.2023)
42. M.King, M.Dworzanowski. In *NI 43-101 Technical Report*. (Neo Lithium corp., Catamarca, Argentina, 2021). pp. 368; https://minedocs.com/21/Tres-Quebradas-FS-11252021.pdf (access date 07.04.2023)
43. V.Flexer, C.F.Baspineiro, C.I.Galli. *Sci. Total Environ.*, **639**, 1188 (2018); https://doi.org/10.1016/j.scitotenv.2018.05.223
44. F.Reidel, P.Ehren, M.Dworzanowski. In *NI 43-101 Technical report*. (Atacama Water and Worley, Chile, 2022). pp. 416; https://lithiumpowerinternational.com/wp-content/uploads/2022/01/NI43-101_DFS2022_LR.pdf (access date 07.04.2023)
45. M.Yu, B.Bai, S. Xiong, X.Liao. *J. Clean. Prod.*, **321**, 128935 (2021); https://doi.org/10.1016/j.jclepro.2021.128935
46. Y.Chen, Y.Kang, Y.Zhao, L.Wang, J.Liu, Y.Li, Z.Liang, X.He, X.Li, N.Tavajohi, B.Li. *J. Energy Chem.*, **59**, 83 (2021); https://doi.org/10.1016/j.jechem.2020.10.017
47. X.Zhang, Y.Xie, X.Lin, H.Li, H.Cao. *J. Mater. Cycles Waste Manag.*, **15**, 420 (2013); https://doi.org/10.1007/s10163-013-0140-y
48. C.Peng, F.Liu, Z.Wang, B.P.Wilson, M.Lundström. *J. Power Sources*, **415**, 179 (2019); https://doi.org/10.1016/j.jpowsour.2019.01.072
49. Y.Zhao, T.Rüther, J.Staines. In *Technical Report*. (CSIRO, Australia, 2021). P. 111; https://www.researchgate.net/profile/Yanyan-Zhao-8/publication/350342227_Australian_landscape_for_lithium-ion_battery_recycling_and_reuse_in_2020_CURRENT_STATUS_GAP_ANALYSIS_AND_INDUSTRY_PERSPECTIVES_Produced_for_the_Future_Battery_Industries_CRC/links/605ab41e458515e83467fb46/Australian-landscape-for-lithium-ion-battery-recycling-and-reuse-in-2020-CURRENT-STATUS-GAP-ANALYSIS-AND-INDUSTRY-PERSPECTIVES-Produced-for-the-Future-Battery-Industries-CRC.pdf
50. N.Bhandari, A.Cai, K.Yuzawa, J.Zhang, V.Joshi, F.Fang, G.Lee, R.Harada, S.Shin. In *Technical Report*. (The Goldman Sachs Group, USA, 2022). P. 33; https://www.goldmansachs.com/insights/pages/gs-research/batteries-the-greenflation-challenge/report.pdf
51. S.Al-Thyabat, T.Nakamura, E.Shibata, A.Iizuka. *Miner. Eng.*, **45**, 4 (2013); https://doi.org/10.1016/j.mineng.2012.12.005
52. O.Velázquez-Martínez, J.Valio, A.Santasalo-Aarnio, M.Reuter, R.Serna-Guerrero. *Batteries*, **5**, 68 (2019); https://doi.org/10.3390/batteries5040068
53. G.J.Doornbusch, M.Tedesco, J.W.Post, Z.Borneman, K.Nijmeijer. *Desalination*, **464**, 105 (2019); https://doi.org/10.1016/j.desal.2019.04.025
54. N.Jacquet, S.Wurtzer, G.Darracq, Y.Wyart, L.Moulin, P.Moulin. *J. Membr. Sci.*, **634**, 119417 (2021); https://doi.org/10.1016/j.memsci.2021.119417
55. N.N.R.Ahmad, W.L.Ang, C.P.Leo, A.W.Mohammad, N.Hilal. *Desalination*, **517**, 115170 (2021); https://doi.org/10.1016/j.desal.2021.115170
56. M.Elimelech, W.A.Phillip. *Science*, **333**, 712 (2011); https://doi.org/10.1126/science.1200488
57. W.-H.Zhang, M.-J.Yin, Q.Zhao, C.-G.Jin, N.Wang, S.Ji, C.L.Ritt, M.Elimelech, Q.-F.An. *Nat. Nanotechnol.*, **16**, 337 (2021); https://doi.org/10.1038/s41565-020-00833-9
58. H.Strathmann. *Desalination*, **264**, 268 (2010); https://doi.org/10.1016/j.desal.2010.04.069
59. A.W.Mohammad, Y.H.Teow, W.L.Ang, Y.T.Chung, D.L.Oatley-Radcliffe, N.Hilal. *Desalination*, **356**, 226 (2015); https://doi.org/10.1016/j.desal.2014.10.043
60. P.Y.Apel, O.V.Bobreshova, A.V.Volkov, V.V.Volkov, V.V.Nikonenko, I.A.Stenina, A.N.Filippov, Y.P.Yampolskii, A.B.Yaroslavtsev. *Membr. Membr. Technol.*, **1**, 45 (2019); https://doi.org/10.1134/S2517751619020021
61. C.Li, D.L.Ramasamy, M.Sillanpää, E.Repo. *Sep. Purif. Technol.*, **254**, 117442 (2021); https://doi.org/10.1016/j.carbpol.2020.117442
62. J.-M.AranaJuve, F.M.S.Christensen, Y.Wang, Z.Wei. *Chem. Eng. J.*, **435**, 134857 (2022); https://doi.org/10.1016/j.cej.2022.134857
63. H.B.Park, J.Kamcev, L.M.Robeson, M.Elimelech, B.D.Freeman. *Science*, **356**, eaab0530 (2017); https://doi.org/10.1126/science.aab0530
64. B.E.Logan, M.Elimelech. *Nature (London)*, **488**, 313 (2012); https://doi.org/10.1038/nature11477
65. J.R.Varcoe, P.Atanassov, D.R.Dekel, A.M.Herring, M.A.Hickner, P.A.Kohl, A.R.Kucernak, W.E.Mustain, K.Nijmeijer, K.Scott, T.Xu, L.Zhuang. *Energy Environ. Sci.*, **7**, 3135 (2014); https://doi.org/10.1039/C4EE01303D
66. A.Y.Alent'ev, A.V.Volkov, I.V.Vorotyntsev, A.L.Maksimov, A.B.Yaroslavtsev. *Membr. Technol.*, **3**, 255 (2021); https://doi.org/10.1134/S2517751621050024
67. A.Yaksic, J.E.Tilton. *Resour. Policy*, **34**, 185 (2009); https://doi.org/10.1016/j.resourpol.2009.05.002
68. T.Sata, T.Sata, M.Yang. *J. Membr. Sci.*, **206**, 31 (2002); https://doi.org/10.1016/S0376-7388(01)00491-4
69. W.Wang, R.Liu, M.Tan, H.Sun, Q.J.Niu, T.Xu, V.Nikonenko,Y.Zhang. *J. Membr. Sci.*, **582**, 236 (2019); https://doi.org/10.1016/j.memsci.2019.04.007

70. F.G.Helfferich. In *Ion Exchange*. (NewYork: McGraw-Hill, 1962). P. 465; https://books.google.ru/books?hl=ru&lr=&id=-F9OQMEA88CAC&oi=fnd&pg=PA1&dq=F.G.+Helfferich+Ion+Exchange+1962&ots=848ETU_P1x&sig=yCjHGOuhX57-REDpVzOw_urIRl78&redir_esc=y#v=onepage&q&f=false
71. K.Kontturi, L.Murtomäki, J.A.Manzanares. In *Electrochemistry and Membrane Science*. (Oxford University Press, 2008). P. 304; https://doi.org/10.1093/acprof:oso/9780199533817.001.0001
72. S.-T.Hwang, K.Kammermeyer. In *Electromembrane Processes Membranes in Separation. Techniques of Chemistry*. (New York: McGraw-Hill, 1975). P. 559
73. V.I.Zabolotskii, V.V.Nikonenko. In *Ion Transport in Membranes*. (Moscow: Nauka, 1996). P. 390; https://echemistry.ru/literatura/prochee/zabolockij-v.i.-nikonenko-v.v.-perenos-ionov-v-membranah.-m.-nauka-1996.-392-s.html
74. D.Y.Butylskii, N.D.Pismenskaya, P.Y.Apel, K.G.Sabbatovskiy, V.V.Nikonenko. *J. Membr. Sci.*, **635**, 119449 (2021); https://doi.org/10.1016/j.memsci.2021.119449
75. N.Pismenskaya, N.Melnik, E.Nevakshenova, K.Nebavskaya, V.Nikonenko*Int. J. Chem. Eng.*, **2012**, 1, 170 (2012); https://doi.org/10.1155/2012/528290
76. H.Strathmann. In *Membrane Science and Technology*. (The Nederlands: Elsevier Science, 2004). P. 360; https://books.google.ru/books?hl=ru&lr=&id=pcNF7HWbFPIC&oi=fnd&pg=PP1&ots=SMZ400_AYD&sig=BzeW8Mfwz8iCH1nzB_AgljQOuLQ&redir_esc=y#v=onepage&q&f=false
77. S.Burn, M.Hoang, D.Zarzo, F.Olewniak, E.Campos, B.Bolto, O.Barron. *Desalination*, **364**, 2 (2015); https://doi.org/10.1016/j.desal.2015.01.041
78. X.Li, C.Zhang, S.Zhang, J.Li, B.He, Z.Cui. *Desalination*, **369**, 26 (2015); https://doi.org/10.1016/j.desal.2015.04.027
79. Y.Xu, H.Peng, H.Luo, Q.Zhang, Z.Liu, Q.Zhao. *Desalination*, **526**, 115519 (2022); https://doi.org/10.1016/j.desal.2021.115519
80. M.A.Ashraf, J.Wang, B.Wu, P.Cui, B.Xu, X.Li *J. Appl. Polym. Sci.*, **137**, 49549 (2020); https://doi.org/10.1002/app.49549
81. https://www.sterlitech.com/flat-sheet-membranes.html (access date 22.01.2023)
82. Y.-F.Zhang, L.Liu, J.Du, R.Fu, B.Van der Bruggen, Y.Zhang. *J. Membr. Sci.*, **523**, 385 (2017); https://doi.org/10.1016/j.memsci.2016.09.052
83. H.-Z.Zhang, Z.-L.Xu, H.Ding, Y.-J.Tang. *Desalination*, **420**, 158 (2017); https://doi.org/10.1016/j.desal.2017.07.011
84. Y.Mizutani. *J. Membr. Sci.*, **54**, 233 (1990); https://doi.org/10.1016/S0376-7388(00)80612-2
85. F.Sheng, N.U.Afsar, Y.Zhu, L.Ge, T.Xu. *Membranes*, **10**, 114 (2020); https://doi.org/10.3390/membranes10060114
86. T.Sata, K.Mine, M.Higa. *J. Membr. Sci.*, **141**, 137 (1998); https://doi.org/10.1016/S0376-7388(97)00296-2
87. T.Sata. *J. Membr. Sci.*, **167**, 1 (2000); https://doi.org/10.1016/S0376-7388(99)00277-X
88. I.Louati, F.Guesmi, C.Hannachi, B.Hamrouni. *Can. J. Chem. Eng.*, **94**, 2386 (2016); https://doi.org/10.1002/cjce.22615
89. J.Pan, J.Ding, R.Tan, G.Chen, Y.Zhao, C.Gao, B.V.der Bruggen, J.Shen. *J. Membr. Sci.*, **539**, 263 (2017); https://doi.org/10.1016/j.memsci.2017.06.017
90. A.Somrani, A.H.Hamzaoui, M.Pontie. *Desalination*, **317**, 184 (2013); https://doi.org/10.1016/j.desal.2013.03.009
91. D.Zhang, Y.Wang, X.Wang, B.Chen, Y.Wang, C.Jiang, T.Xu. *Chem. Eng. Sci.*, **245**, 116873 (2021); https://doi.org/10.1016/j.ces.2021.116873
92. D.Lu, T.Ma, S.Lin, Z.Zhou, G.Li, Q.An, Z.Yao, Q.Sun, Z.Sun, L.Zhang. *J. Membr. Sci.*, **635**, 119504 (2021); https://doi.org/10.1016/j.memsci.2021.119504
93. F.Soyekwo, H.Wen, D.Liao, C.Liu. *ACS Appl. Mater. Interfaces*, **14**, 32420 (2022); https://doi.org/10.1021/acsami.2c03650
94. P.Xu, J.Hong, X.Qian, Z.Xu, H.Xia, Q.-Q.Ni. *Desalination*, **488**, 114522 (2020); https://doi.org/10.1016/j.desal.2020.114522
95. P.Xu, J.Hong, Z.Xu, H.Xia, Q.-Q.Ni. *Sep. Purif. Technol.*, **270**, 118796 (2021); https://doi.org/10.1016/j.seppur.2021.118796
96. C.Guo, N.Li, X.Qian, J.Shi, M.Jing, K.Teng, Z.Xu. *Sep. Purif. Technol.*, **230**, 115567 (2020); https://doi.org/10.1016/j.seppur.2019.05.009
97. W.Li, C.Shi, A.Zhou, X.He, Y.Sun, J.Zhang. *Sep. Purif. Technol.*, **186**, 233 (2017); https://doi.org/10.1016/j.seppur.2017.05.044
98. H.Peng, Q.Zhao. *Adv. Funct. Mater.*, **31**, 2009430 (2021); https://doi.org/10.1002/adfm.202009430
99. H.Strathmann. In *Ullmann's Encyclopedia of Industrial Chemistry*. Wiley, Weinheim, Germany, 2011. P. 413; https://doi.org/10.1002/14356007.a16_187.pub3
100. T.Sata. *J. Membr. Sci.*, **93**, 117 (1994); https://doi.org/10.1016/0376-7388(94)80001-4
101. X.-Y. Nie, S.-Y.Sun, Z.Sun, X.Song, J.-G.Yu. *Desalination*, **403**, 128 (2017); https://doi.org/10.1016/j.desal.2016.05.010
102. M.Galizia, F.M.Benedetti, D.R.Paul, B.D.Freeman. *J. Membr. Sci.*, **535**, 132 (2017); https://doi.org/10.1016/j.memsci.2017.04.007
103. C.Zhao, J.Zhang, G.He, T.Wang, D.Hou, Z.Luan. *Chem. Eng. J.*, **233**, 224 (2013); https://doi.org/10.1016/j.cej.2013.08.027
104. T.Bello, Z.Slouka. *J. Membr. Sci.*, **610**, 118291 (2020); https://doi.org/10.1016/j.memsci.2020.118291
105. V.D.Titorova, I.A.Moroz, S.A.Mareev, N.D.Pismenskaya, K.G.Sabbatovskii, Y.Wang, T.Xu, V.V.Nikonenko. *J. Membr. Sci.*, **644**, 120149 (2022); https://doi.org/10.1016/j.memsci.2021.120149
106. N.White, M.Misovich, A.Yaroshchuk, M.L.Bruening. *ACS Appl. Mater. Interfaces*, **7**, 6620 (2015); https://doi.org/10.1021/am508945p
107. T.Luo, S.Abdu, M.Wessling. *J. Membr. Sci.*, **555**, 429 (2018); https://doi.org/10.1016/j.memsci.2018.03.051
108. V.I.Zabolotsky, A.R.Achoh, K.A.Lebedev, S.S.Melnikov. *J. Membr. Sci.*, **608**, 118152 (2020); https://doi.org/10.1016/j.memsci.2020.118152
109. S.Abdu, M.-C.Martí-Calatayud, J.E.Wong, M.García-Gabaldón, M.Wessling. *ACS Appl. Mater. Interfaces*, **6**, 1843 (2014); https://doi.org/10.1021/am4048317
110. E.Evdochenko, J.Kamp, R.Femmer, Y.Xu, V.V.Nikonenko, M.Wessling. *J. Membr. Sci.*, **611**, 118045 (2020); https://doi.org/10.1016/j.memsci.2020.118045
111. L.Paltrinieri, K.Remmen, B.Müller, L.Chu, J.Köser, T.Wintgens, M.Wessling, L.C.P.MdeSmet, E.J.R. Sudhölter. *J. Membr. Sci.*, **587**, 117162 (2019); https://doi.org/10.1016/j.memsci.2019.06.002
112. G.Saracco. *Chem. Eng. Sci.*, **52**, 3019 (1997); https://doi.org/10.1016/S0009-2509(97)00107-3
113. Y.Zhao, K.Tang, Q.Liu, B.VanderBruggen, A.S.Díaz, J.Pan, C.Gao, J.Shen. *RSC Adv.*, **6**, 16548 (2016); https://doi.org/10.1039/C5RA27916J
114. J.Moreno, V.Díez, M.Saakes, K.Nijmeijer. *J. Membr. Sci.*, **550**, 155 (2018); https://doi.org/10.1016/j.memsci.2017.12.069
115. J.Ying, M.Luo, Y.Jin, J.Yu. *Desalination*, **492**, 114621 (2020); https://doi.org/10.1016/j.desal.2020.114621
116. X.-C.Zhang, J.Wang, Z.-Y.Ji, P.-Y.Ji, J.Liu, Y.-Y.Zhao, F.Li, J.-S.Yuan. *J. Environ. Chem. Eng.*, **9**, 106635 (2021); https://doi.org/10.1016/j.jece.2021.106635
117. P.-Y.Ji, Z.-Y.Ji, Q.-B.Chen, J.Liu, Y.-Y.Zhao, S.-Z.Wang, F.Li, J.-S.Yuan. *Sep. Purif. Technol.*, **207**, 1 (2018); https://doi.org/10.1016/j.seppur.2018.06.012
118. Y.Qiu, H.Ruan, C.Tang, L.Yao, J.Shen, A.Sotto. *ACS Sustain. Chem. Eng.*, **7**, 13481 (2019); https://doi.org/10.1021/acssuschemeng.9b03108
119. Y.Zhou, H.Yan, X.Wang, L.Wu, Y.Wang, T.Xu. *Desalination*, **425**, 30 (2018); https://doi.org/10.1016/j.desal.2017.10.013

120. G.Martin, A.Schneider, W.Voigt, M.Bertau. *Miner. Eng.*, **110**, 75 (2017); https://doi.org/10.1016/j.mineng.2017.04.009
121. K.H.Chan, M.Malik, G.Azimi. *Resour. Conserv. Recycl.*, **178**, 106076 (2022); https://doi.org/10.1016/j.resconrec.2021.106076
122. S.Gmar, A.Chagnes, F.Lutin, L.Muhr. *Recycling*, **7**, 14 (2022); https://doi.org/10.3390/recycling7020014
123. A.Siekierka, F.Yalcinkaya. *Sep. Purif. Technol.*, **299**, 121695 (2022); https://doi.org/10.1016/j.seppur.2022.121695
124. Y.Song, Z.Zhao*Sep. Purif. Technol.*, **206**, 335 (2018); https://doi.org/10.1016/j.seppur.2018.06.022
125. M.Shi, L.A.Diaz, J.R.Klaehn, A.D.Wilson, T.E.Lister. *ACS Sustain. Chem. Eng.*, **10**, 11773 (2022); https://doi.org/10.1021/acssuschemeng.2c02106
126. E.Güler, W.vanBaak, M.Saakes, K.Nijmeijer. *J. Membr. Sci.*, **455**, 254 (2014); https://doi.org/10.1016/j.memsci.2013.12.054
127. L.Ge, B.Wu, D.Yu, A.N.Mondal, L.Hou, N.U.Afsar, Q.Li, T.Xu, J.Miao, T.Xu*Chinese. J. Chem. Eng.*, **25**, 1606 (2017); https://doi.org/10.1016/j.cjche.2017.06.002
128. D.V.Golubenko, Y.A.Karavanova, S.S.Melnikov, A.R.Achoh, G.Pourcelly, A.B.Yaroslavtsev. *J. Membr. Sci.*, **563**, 777 (2018); https://doi.org/10.1016/j.memsci.2018.06.024
129. M.Ahmad, A.Yaroshchuk, M.L.Bruening. *J. Membr. Sci.*, **616**, 118570 (2020); https://doi.org/10.1016/j.memsci.2020.118570
130. W.Jiang, L.Lin, X.Xu, H.Wang, P.Xu. *J. Membr. Sci.*, **572**, 545 (2019); https://doi.org/10.1016/j.memsci.2018.11.038
131. J.Balster, O.Krupenko, I.Punt, D.Stamatialis, M.Wessling. *J. Membr. Sci.*, **263**, 137 (2005); https://doi.org/10.1016/j.memsci.2005.04.019
132. J.Kerres, W.Cui, R.Disson, W.Neubrand. *J. Membr. Sci.*, **139**, 211 (1998); https://doi.org/10.1006/jssc.1998.7952
133. I.Ali, M.A.Raza, R.Mehmood, A.Islam, A.Sabir, N.Gull, B.Haider, S.H.Park, R.U.Khan. *Int. J. Mol. Sci.*, **21**, 7338 (2020); https://doi.org/10.3390/ijms21197338
134. T.Chakrabarty, M.Kumar, K.P.Rajesh, V.K.Shahi, T.S.Natarajan. *Sep. Purif. Technol.*, **75**, 174 (2010); https://doi.org/10.1016/j.seppur.2010.07.019
135. D.V.Golubenko, R.R.Shaydullin, A.B.Yaroslavtsev. *Colloid Polym. Sci.*, **297**, 741 (2019); https://doi.org/10.1007/s00396-019-04499-1
136. I.Stenina, D.Golubenko, V.Nikonenko, A.Yaroslavtsev. *Int. J. Mol. Sci.*, **21**, 5517 (2020); https://doi.org/10.3390/ijms21155517
137. Y.Zhao, Y.Liu, C.Wang, E.Ortega, X.Wang, Y.F.Xie, J.Shen, C.Gao, B.VanderBruggen. *J. Mater. Chem. A*, **8**, 4244 (2020); https://doi.org/10.1039/C9TA13247C
138. N.U.Afsar, M.A.Shehzad, M.Irfan, K.Emmanuel, F.Sheng, T.Xu, X.Ren, L.Ge, T.Xu. *Desalination*, **458**, 25 (2019); https://doi.org/10.1016/j.desal.2019.02.004
139. M.B.Bajestani, A.Moheb, M.Dinari. *Desalination*, **486**, 114476 (2020); https://doi.org/10.1016/j.desal.2020.114476
140. Z.Zhao, G.Liu, H.Jia, L.He. *J. Membr. Sci.*, **596**, 117685 (2020); https://doi.org/10.1016/j.memsci.2019.117685
141. G.Zante, M.Boltoeva, A.Masmoudi, R.Barillon, D.Trébouet. *J. Membr. Sci.*, **580**, 62 (2019); https://doi.org/10.1016/j.memsci.2019.03.013
142. Z.Qian, H.Miedema, S.Sahin, L.C.P.M.deSmet, E.J.R.Sudhölter. *Desalination*, **495**, 114631 (2020); https://doi.org/10.1016/j.desal.2020.114631
143. E.P.Horwitz, R.Chiarizia, H.Diamond, R.C.Gatrone, S.D.Alexandratos, A.Q.Trochimczuk, D.W.Crick. *Solv. Extr. Ion Exch.*, **11**, 943 (1993); https://doi.org/10.1080/07366299308918195
144. A.Münchinger, K.-D.Kreuer. *J. Membr. Sci.*, **592**, 117372 (2019); https://doi.org/10.1016/j.memsci.2019.117372
145. H.J.Cassady, E.C.Cimino, M.Kumar, M.A.Hickner. *J. Membr. Sci.*, **508**, 146 (2016); https://doi.org/10.1016/j.memsci.2016.02.048
146. T.Hoshino. *Desalination*, **359**, 59 (2015); https://doi.org/10.1016/j.desal.2014.12.018
147. T.Ounissi, L.Dammak, C.Larchet, J.-F.Fauvarque, E.S.B.H.Hmida. *J. Mater. Sci.*, **55**, 16111 (2020); https://doi.org/10.1007/s10853-020-05147-8
148. T.Ounissi, R.B.Ammar, C.Larchet, L.Chaabane, L.Baklouti, L.Dammak, E.S.B.H.Hmida. *Membranes*, **12**, 244 (2022); https://doi.org/10.3390/membranes12020244
149. X.Yan, S.Anguille, M.Bendahan, P.Moulin. *Sep. Purif. Technol.*, **222**, 230 (2019); https://doi.org/10.1016/j.seppur.2019.03.103
150. M.A.Malik, M.A.Hashim, F.Nabi. *Chem. Eng. J.*, **171**, 242 (2011); https://doi.org/10.1016/j.cej.2011.03.041
151. A.J.B.Kemperman, D.Bargeman, T.V.D.Boomgaard, H.Strathmann. *Sep. Sci. Technol.*, **31**, 2733 (1996); https://doi.org/10.1080/01496399608000824
152. A.Razmjou, G.Eshaghi, Y.Orooji, E.Hosseini, A.H.Korayem, F.Mohagheghian, Y.Boroumand, A.Noorbakhsh, M.Asadnia, V.Chen. *Water Res.*, **159**, 313 (2019); https://doi.org/10.1016/j.watres.2019.05.018
153. H.Zhang, J.Hou, Y.Hu, P.Wang, R.Ou, L.Jiang, J.Z.Liu, B.D.Freeman, A.J.Hill, H.Wang. *Sci. Adv.*, **4**, (2018); https://doi.org/10.1126/sciadv.aar6782
154. P.P.Sharma, V.Yadav, A.Rajput, H.Gupta, H.Saravaia, V.Kulshrestha. *Desalination*, **496**, 114755 (2020); https://doi.org/10.1016/j.desal.2020.114755
155. A.González, M.Grágeda, A.Quispe, S.Ushak, P.Sistat, M.Cretin. *Membranes*, **11**, 575 (2021); https://doi.org/10.3390/membranes11080575
156. R.Pärnamäe, S.Mareev, V.Nikonenko, S.Melnikov, N.Sheldeshov, V.Zabolotskii, H.V.M.Hamelers, M.Tedesco. *J. Membr. Sci.*, **617**, 118538 (2021); https://doi.org/10.1016/j.memsci.2020.118538
157. Y.Zhao, X.Xiang, M.Wang, H.Wang, Y.Li, J.Li, H.Yang. *Desalination*, **512**, 115126 (2021); https://doi.org/10.1016/j.desal.2021.115126
158. D.İpekçi, N.Kabay, S.Bunani, E.Altıok, M.Arda, K.Yoshizuka, S.Nishihama. *Desalination*, **479**, 114313 (2020); https://doi.org/10.1016/j.desal.2020.114313
159. S.Bunani, K.Yoshizuka, S.Nishihama, M.Arda, N.Kabay. *Desalination*, **424**, 37 (2017); https://doi.org/10.1016/j.desal.2017.09.029
160. W.R.Torres, C.H.D.Nieto, A.Prévoteau, K.Rabaey, V.Flexer. *J. Membr. Sci.*, **615**, 118416 (2020); https://doi.org/10.1016/j.memsci.2020.118416
161. C.H.D.Nieto, K.Rabaey, V.Flexer. *Sep. Purif. Technol.*, **252**, 117410 (2020); https://doi.org/10.1016/j.seppur.2020.117410
162. P.Agarwal, I.Tomlinson, R.E.Hefner, S.Ge, Y.Rao, T.Dikic. *J. Membr. Sci.*, **572**, 475 (2019); https://doi.org/10.1016/j.memsci.2018.11.028
163. V.Freger *Environ. Sci. Technol.*, **38**, 3168 (2004); https://doi.org/10.1021/es034815u
164. S.Bason, Y.Oren, V.Freger. *J. Membr. Sci.*, **367**, 119 (2011); https://doi.org/10.1016/j.memsci.2010.10.048
165. A.Yaroshchuk, M.L.Bruening, E.E.LicónBernal. *J. Membr. Sci.*, **447**, 463 (2013); https://doi.org/10.1016/j.memsci.2013.07.047
166. A.Yaroshchuk. *Sep. Purif. Technol.*, **22**–**23**, 143 (2001); https://doi.org/10.1016/S1383-5866(00)00159-3
167. D.L.Oatley-Radcliffe, M.Walters, T.J.Ainscough, P.M.Williams, A.W.Mohammad, N.Hilal. *J. Water Process Eng.*, **19**, 164 (2017); https://doi.org/10.1016/j.jwpe.2017.07.026
168. P.M.Biesheuvel, S.Porada, M.Elimelech, J.E.Dykstra. *J. Membr. Sci.*, **647**, 120221 (2022); https://doi.org/10.1016/j.memsci.2021.120221
169. V.V.Nikonenko, A.B.Yaroslavtsev, G.Pourcelly. In *Ionic Interactions in Natural and Synthetic Macromolecules*. John Wiley & Sons, 2012. P. 267; https://doi.org/10.1002/9781118165850.ch9
170. X.-L.Wang, T.Tsuru, S.Nakao, S.Kimura. *J. Membr. Sci.*, **135**, 19 (1997); https://doi.org/10.1016/S0192-0561(97)00016-7

171. D.-X.Wang, M.Su, Z.-Y.Yu, X.-L.Wang, M.Ando, T.Shintani. *Desalination*, **175**, 219 (2005); https://doi.org/10.1016/j.desal.2004.10.009
172. A.Szymczyk, P.Fievet. *J. Membr. Sci.*, **252**, 77 (2005); https://doi.org/10.1016/j.memsci.2004.12.002
173. S.Ilyas, R.English, P.Aimar, J.-F.Lahitte, W.M.deVos. *Colloids Surf. A: Phys.-Chem. Eng. Asp.*, **533**, 286 (2017); https://doi.org/10.1016/j.colsurfa.2017.09.003
174. A.Yaroshchuk, M.L.Bruening, E.Zholkovskiy. *Adv. Colloid Interface Sci.*, **268**, 39 (2019); https://doi.org/10.1016/j.cis.2019.03.004
175. R.Wang, S.Lin. *J. Membr. Sci.*, **620**, 118809 (2021); https://doi.org/10.1016/j.memsci.2020.118809
176. V.Fíla, K.Bouzek. *J. Appl. Electrochem.*, **33**, 675 (2003); https://doi.org/10.1023/A:1025018726112
177. M.Tedesco, H.V.M.Hamelers, P.M.Biesheuvel. *J. Membr. Sci.*, **510**, 370 (2016); https://doi.org/10.1016/j.memsci.2016.03.012
178. A.Campione, L.Gurreri, M.Ciofalo, G.Micale, A.Tamburini, A.Cipollina. *Desalination*, **434**, 121 (2018); https://doi.org/10.1016/j.desal.2017.12.044
179. J.Kamcev, R.Sujanani, E.-S.Jang, N.Yan, N.Moe, D.R.Paul, B.D.Freeman. *J. Membr. Sci.*, **547**, 123 (2018); https://doi.org/10.1016/j.memsci.2017.10.024
180. S.Mareev, A.Gorobchenko, D.Ivanov, D.Anokhin, V.Nikonenko. *Int. J. Mol. Sci.*, **24**, 34 (2022); https://doi.org/10.3390/ijms24010034
181. A.E.Yaroshchuk. *Adv. Colloid Interface Sci.*, **85**, 193 (2000); https://doi.org/10.1016/S0001-8686(99)00021-4
182. A.Moliton. In *Basic Electromagnetism and Materials*. (New York: Springer, 2007). P. 39; https://picture.iczhiku.com/resource/eetop/ShiyazkGGeZurCvc.pdf
183. S.Bandini, D.Vezzani. *Chem. Eng. Sci.*, **58**, 3303 (2003); https://doi.org/10.1016/S0009-2509(03)00212-4 (access date 07.04.2023)
184. E.Glueckauf. In *Proceeding of the First International Symposium on Water Desalination*. (Washington, 1965). P. 143; https://books.google.ru/books?id=JChow5kkCmYC&printsec=frontcover&hl=ru&source=gbs_ge_summary_r&cad=0#v=onepage&q&f=false (access date 07.04.2023)
185. M.S.Hall, V.N.Starov, D.R.Lloyd. *J. Membr. Sci.*, **128**, 23 (1997); https://doi.org/10.1016/S0376-7388(96)00300-6
186. R.Vacassy. *J. Membr. Sci.*, **132**, 109 (1997); https://doi.org/10.1016/S0376-7388(97)00051-3
187. J.Schaep. *Sep. Purif. Technol.*, **22 – 23**, 169 (2001); https://doi.org/10.1016/S1383-5866(00)00163-5
188. A.Szymczyk, H.Zhu, B.Balannec. *J. Phys. Chem. B*, **114**, 10143 (2010); https://doi.org/10.1021/jp1025575
189. Y.I.Dirir, Y.Hanafi, A.Ghoufi, A.Szymczyk. *Langmuir*, **31**, 451 (2015); https://doi.org/10.1021/la5044188
190. A.Yaroshchuk, Y.Zhu, M.Bondarenko, M.L.Bruening. *Langmuir*, **32**, 2644 (2016); https://doi.org/10.1021/acs.langmuir.5b04588
191. O.Kedem, A.Katchalsky. *Trans. Faraday Soc.*, **59**, 1918 (1963); https://doi.org/10.1039/TF9635901918
192. S.Koter. *Desalination*, **198**, 335 (2006); https://doi.org/10.1016/j.desal.2006.02.009
193. K.S.Spiegler, O.Kedem. *Desalination*, **1**, 311 (1966); https://doi.org/10.1016/S0011-9164(00)80018-1
194. O.Kedem, V.Freger. *J. Membr. Sci.*, **310**, 586 (2008); https://doi.org/10.1016/j.memsci.2007.11.045
195. A.E.Yaroshchuk. *J. Membr. Sci.*, **198**, 285 (2002); https://doi.org/10.1016/S0376-7388(01)00668-8
196. A.Filippov, T.Philippova. *Colloids Interfaces*, **6**, 34 (2022); https://doi.org/10.3390/colloids6020034
197. J.Happel, H.Brenner. In *Mechanics of Fluids and Transport Processes*. (The Netherlands: Martinus Nijhoff Publishers, 1991). P. 564; https://link.springer.com/book/10.1007/978-94-009-8352-6
198. A.N.Filippov. *Colloid J.*, **80**, 716 (2018); https://doi.org/10.1134/S1061933X18060030
199. A.N.Filippov. *Colloid J.*, **80**, 728 (2018); https://doi.org/10.1134/S1061933X18060042
200. A.N.Filippov. *Colloid J.*, **84** 332 – 43 (2022); https://doi.org/10.1134/S1061933X2203005X
201. A.N.Filippov, S.A.Shkirskaya. *Colloid J.*, **81** 597 (2019); https://doi.org/10.1134/S1061933X19050041
202. A.N.Filippov, N.A.Kononenko, N.V.Loza, D.S.Kopitsyn, D.A.Petrova. *Electrochim. Acta*, **389**, 138768 (2021); https://doi.org/10.1016/j.electacta.2021.138768
203. A.N.Filippov, Y.O.Koroleva, A.K.Verma. *Membr. Membr. Technol.*, **2**, 230 (2020); https://doi.org/10.1134/S2517751620040058
204. A.N.Filippov, T.S.Philippova. *Membr. Membr. Technol.*, **3** 15 (2021); https://doi.org/10.1134/S2517751621010066
205. Z.V.P.Murthy, L.B.Chaudhari. *Chem. Eng. J.*, **150**, 181 (2009); https://doi.org/10.1016/j.cej.2008.12.023
206. H.Kelewou, A.Lhassani, M.Merzouki, P.Drogui, B.Sellamuthu. *Desalination*, **277**, 106 (2011); https://doi.org/10.1016/j.desal.2011.04.010
207. Z.Kovács, M.Discacciati, W.Samhaber. *J. Membr. Sci.*, **332**, 38 (2009); https://doi.org/10.1016/j.memsci.2009.01.034
208. A.M.Hidalgo, G.León, M.Gómez, M.D.Murcia, E.Gómez, J.A.Macario. *Membranes*, **10**, 408 (2020); https://doi.org/10.3390/membranes10120408
209. F.Wu, L.Feng, L.Zhang. *Desalination*, **362**, 11 (2015); https://doi.org/10.1016/j.desal.2015.01.046
210. Y.Zhang, L.Zhang, L.Hou, S.Kuang, A.Yu. *AIChE J.*, **65**, 1076 (2019); https://doi.org/10.1002/aic.16475
211. B.DeJaegher, W.DeSchepper, A.Verliefde, I.Nopens. *J. Membr. Sci.*, **642**, 119975 (2022); https://doi.org/10.1016/j.memsci.2021.119975
212. P.Y.Apel, S.Velizarov, A.V.Volkov, T.V.Eliseeva, V.V.Nikonenko, A.V.Parshina, N.D.Pismenskaya, K.I.Popov, A.B.Yaroslavtsev. *Membr. Membr. Technol.*, **4**, 69 (2022); https://doi.org/10.1134/S2517751622020032
213. R.Femmer, A.Mani, M.Wessling. *Sci. Rep.*, **5**, 11583 (2015); https://doi.org/10.1038/srep11583
214. R.Femmer, M.C.Martí-Calatayud, M.Wessling. *J. Memb. Sci.*, **520**, 29 (2016); https://doi.org/10.1016/j.memsci.2016.07.055
215. E.Evdochenko, J.Kamp, R.Dunkel, V.V.Nikonenko, M.Wessling. *J. Membr. Sci.*, **636**, 119533 (2021); https://doi.org/10.1016/j.memsci.2021.119533
216. H.Zhu, A.Szymczyk, B.Balannec. *J. Membr. Sci.*, **379**, 215 (2011); https://doi.org/10.1016/j.memsci.2011.05.062
217. B.DeJaegher, W.DeSchepper, A.Verliefde, I.Nopens. *Sep. Purif. Technol.*, **259**, 118028 (2021); https://doi.org/10.1016/j.seppur.2020.118028
218. M.K.Urtenov, A.M.Uzdenova, A.V.Kovalenko, V.V.Nikonenko, N.D.Pismenskaya, V.I.Vasil'eva, P.Sistat, G.Pourcelly. *J. Membr. Sci.*, **447**, 190 (2013); https://doi.org/10.1016/j.memsci.2013.07.033
219. W.R.Bowen, M.G.Jones, J.S.Welfoot, H.N.S.Yousef. *Desalination*, **129**, 147 (2000); https://doi.org/10.1016/S0011-9164(00)00057-6
220. G.Jing, W.Du, Y.Guo. *Desalination*, **291**, 78 (2012); https://doi.org/10.1016/j.desal.2012.02.002
221. M.Asghari, A.Dashti, M.Rezakazemi, E.Jokar, H.Halakoei. *Rev. Chem. Eng.*, **36**, 265 (2020); https://doi.org/10.1515/revce-2018-0011
222. J.Jawad, A.H.Hawari, S.J.Zaidi. *Chem. Eng. J.*, **419**, 129540 (2021); https://doi.org/10.1016/j.cej.2021.129540
223. D.Rall, D.Menne, A.M.Schweidtmann, J.Kamp, L.V.Kolzenberg, A.Mitsos, M.Wessling. *J. Membr. Sci.*, **569**, 209 (2019); https://doi.org/10.1016/j.memsci.2018.10.013
224. D.Rall, A.M.Schweidtmann, M.Kruse, E.Evdochenko, A.Mitsos, M.Wessling. *J. Membr. Sci.*, **608**, 118208 (2020); https://doi.org/10.1016/j.memsci.2020.118208

225. H.Al-Zoubi, N.Hilal, N.A.Darwish, A.W.Mohammad. *Desalination*, **206**, 42 (2007); https://doi.org/10.1016/j.desal.2006.02.060
226. B.DeJaegher, E.Larumbe, W.DeSchepper, A.Verliefde, I.Nopens. *Sep. Purif. Technol.*, **249**, 116939 (2020); https://doi.org/10.1016/j.seppur.2020.116939
227. Y.Oren, A.Litan. *J. Phys. Chem.*, **78**, 1805 (1974); https://doi.org/10.1021/j100611a007
228. V.V.Nikonenko, V.I.Zabolotskii, N.P.Gnusin. *Sov. Electrochem.*, **16**, 472 (1980); https://doi.org/10.1049/el:19800332
229. S.Mafé, V.M.Aguilella, J.Pellicer. *J. Membr. Sci.*, **36**, 497 (1988); https://doi.org/10.1016/0376-7388(88)80039-5
230. N.A.Mishchuk, S.V.Verbich, F.Gonzales-Caballero. *Colloid J.*, **63**, 586 (2001); https://doi.org/10.1023/A:1012399018946
231. M.I.Ponomarev, L.K.Zhiginas, R.D.Chebotareva, V.D.Grebenyuk. *Elektrokhimiya*, **19**, 387 (1983); https://doi.org/10.1016/0376-4583(83)90044-4
232. A.Chapotot, G.Pourcelly, C.Gavach. *J. Membr. Sci.*, **96**, 167 (1994); https://doi.org/10.1016/0376-7388(94)00107-3
233. G.Pourcelly, P.Sistat, A.Chapotot, C.Gavach, V.Nikonenko. *J. Membr. Sci.*, **110**, 69 (1996); https://doi.org/10.1016/S0033-3506(96)80045-X
234. A.Filippov, D.Afonin, N.Kononenko, Y.Lvov, V.Vinokurov. *Colloids Surfaces A Physicochem. Eng. Asp.*, **521**, 251 (2017); https://doi.org/10.1016/j.colsurfa.2016.08.079
235. I.Y.Kharkats. *Sov. Electrochem.*, **21**, (1986); https://www.osti.gov/biblio/5239221
236. M.A.K.Urtenov, E.V.Kirillova, N.M.Seidova, V.V.Nikonenko. *J. Phys. Chem. B*, **111**, 14208 (2007); https://doi.org/10.1021/jp073103d
237. A.R.Achoh, V.I.Zabolotsky, K.A.Lebedev, M.V.Sharafan, A.B.Yaroslavtsev. *Membr. Membr. Technol.*, **3**, 52 (2021); https://doi.org/10.1134/S2517751621010029
238. D.V.Golubenko, A.B.Yaroslavtsev. *J. Membr. Sci.*, **635**, 119466 (2021); https://doi.org/10.1016/j.memsci.2021.119466
239. A.Gorobchenko, S.Mareev, V.Nikonenko. *Int. J. Mol. Sci.*, **23**, 4711 (2022); https://doi.org/10.3390/ijms23094711
240. A.D.Gorobchenko, V.V.Gil, V.V.Nikonenko, M.V.Sharafan. *Membr. Membr. Technol.*, **4**, 423 (2022); https://doi.org/10.1134/S251775162206004X
241. L.M.Robeson. *J. Membr. Sci.*, **320**, 390 (2008); https://doi.org/10.1016/j.memsci.2008.04.030
242. D.F.Sanders, Z.P.Smith, R.Guo, L.M.Robeson, J.E.McGrath, D.R.Paul, B.D.Freeman. *Polymer*, **54**, 4729 (2013); https://doi.org/10.1016/j.polymer.2013.05.075
243. J.-M.Restrepo-Flórez, M.Maldovan. *Sep. Purif. Technol.*, **228**, 115762 (2019); https://doi.org/10.1016/j.seppur.2019.115762
244. Y.Yampolskii, N.Belov, A.Alentiev. *J. Membr. Sci.*, **598**, 117779 (2020); https://doi.org/10.1016/j.memsci.2019.117779
245. D.V.Golubenko, G.Pourcelly, A.B.Yaroslavtsev. *Sep. Purif. Technol.*, **207**, 329 (2018); https://doi.org/10.1016/j.seppur.2018.06.041
246. G.Zante, M.Boltoeva, A.Masmoudi, R.Barillon, D.Trébouet. *J. Fluor. Chem.*, **236**, 109593 (2020); https://doi.org/10.1016/j.jfluchem.2020.109593
247. S.Yang, F.Zhang, H.Ding, P.He, H.Zhou. *Joule*, **2**, 1648 (2018); https://doi.org/10.1016/j.joule.2018.07.006
248. M.S.Palagonia, D.Brogioli, F.LaMantia. *Desalination*, **475**, 114192 (2020); https://doi.org/10.1016/j.desal.2019.114192
249. T.Ounissi, L.Dammak, J.-F.Fauvarque, E.S.B.H.Hmida. *Sep. Purif. Technol.*, **275**, 119134 (2021); https://doi.org/10.1016/j.seppur.2021.119134
250. H.Kazemzadeh, J.Karimi-Sabet, J.T.Darian, A.Adhami. *Sep. Purif. Technol.*, **251**, 117298 (2020); https://doi.org/10.1016/j.seppur.2020.117298
251. P.Wang, M.Wang, F.Liu, S.Ding, X.Wang, G.Du, J.Liu, P.Apel, P.Kluth, C.Trautmann, Y.Wang. *Nat. Commun.*, **9**, 569 (2018); https://doi.org/10.1038/s41467-017-02344-z
252. Q.Wen, D.Yan, F.Liu, M.Wang, Y.Ling, P.Wang, P.Kluth, D.Schauries, C.Trautmann, P.Apel, W.Guo, G.Xiao, J.Liu, J.Xue, Y.Wang. *Adv. Funct. Mater.*, **26**, 5796 (2016); https://doi.org/10.1002/adfm.201670165
253. Y.I.Dytnerskii, A.E.Savkin, V.D.Sobolev, N.V.Churaev. *Theor. Found. Chem. Eng.*, **15**, 208 (1982)
254. Y.V.Karlin, V.Y.Chuikov, Y.I.Dytnerskii. *Russ. J. Electrochem.*, **32**, 641 (1996); https://www.elibrary.ru/item.asp?id=13244675
255. A.Yaroshchuk. *Membr. Technol.*, **1997**, 5 (1997); https://doi.org/10.1016/S0958-2118(97)85188-9
256. S.Lazarev, S.Kovalev, K.Shestakov. *Acta Period. Technol.*, 236 (2019); https://doi.org/10.2298/APT1950236L
257. S.I.Lazarev, S.V.Kovalev, I.V.Khorokhorina, M.I.Mikhailin. *Chem. Pet. Eng.*, **56**, 475 (2020); https://doi.org/10.1007/s10556-020-00797-6
258. O.Bobreshova, I.Aristov, P.Kulintsov, E.Balavadze. *J. Membr. Sci.*, **177**, 201 (2000); https://doi.org/10.1016/S0376-7388(00)00466-X
259. N.Ishibashi, K.Hirano. *J. Electrochem. Soc. Jpn.*, **27**, E193 (1959); https://doi.org/10.5796/jesj.27.7-9.E193
260. Q.Li, H.Liu, Y.Ji, Z.Cui, F.Yan, M.Younas, J.Li, B.He. *Desalination*, **535**, 115825 (2022); https://doi.org/10.1016/j.desal.2022.115825
261. O.V.Bobreshova, P.I.Kulintsov, I.V.Aristov, E.M.Balavadze. *Russ. J. Electrochem.*, **32**, 164 (1996); https://www.elibrary.ru/item.asp?id=13242966
262. Patent RU 2398618 (2010); https://patents.google.com/patent/RU2398618C2/ru
263. N.V.Shel'deshov, V.V.Chaika, V.I.Zabolotskii. *Russ. J. Electrochem.*, **44**, 1036 (2008); https://doi.org/10.1134/S1023193508090085
264. P.Geng, G.Chen. In *Nanofiltration*. IntechOpen, 2018. P. 133; https://doi.org/10.5772/intechopen.75819
265. H.M.Huotari, G.Trägårdh, I.H.Huisman. *Chem. Eng. Res. Des.*, **77**, 461 (1999); https://doi.org/10.1205/026387699526304
266. S.Lentsch, P.Aimar, J.L.Orozco. *J. Memb. Sci.*, **80**, 221 (1993); https://doi.org/10.1016/0376-7388(93)85146-N
267. L.Ge, B.Wu, Q.Li, Y.Wang, D.Yu, L.Wu, J.Pan, J.Miao, T.Xu. *J. Membr. Sci.*, **498**, 192 (2016); https://doi.org/10.1016/j.memsci.2015.10.001
268. Q.Li, H.Liu, B.He, W.Shi, Y.Ji, Z.Cui, F.Yan, Y.Mohammad, J.Li. *J. Membr. Sci.*, **641**, 119880 (2022); https://doi.org/10.1016/j.memsci.2021.119880
269. A.G.Kislyi, D.Y.Butylskii, S.A.Mareev, V.V. Nikonenko *Membr. Membr. Technol.*, **3**, 131 (2021); https://doi.org/10.1134/S2517751621020062
270. A.K.Brewer, S.L.Madorsky, J.W.Westhaver. *Science*, **104**, 156 (1946); https://doi.org/10.1126/science.104.2694.156
271. A.K.Brewer, S.L.Madorsky, J.K.Taylor, V.H.Dibeler, P.Bradt, O.L.Parham, R.J.Britten, J.G.Reid. *J. Res. Natl. Bur. Stand.*, **38**, 137 (1947); https://doi.org/10.6028/jres.038.005
272. K.Wagener, H.D.Freyer, B.A.Bilal. *Sep. Sci.*, **6**, 483 (1971); https://doi.org/10.1080/00372367108056034
273. L.N.Moskvin, A.N.Katruzov, V.S.Gurskij, P.Y.Apel, V.I.Kuznetsov, V.V.Shirkova. *Dokl. Akad. Nauk SSSR*, **302**, 841 (1988); https://inis.iaea.org/search/search.aspx?orig_q=RN:20028684
274. S.M.Corrêa, G.Arbilla, M.S.Carvalho. *Sep. Sci. Technol.*, **33**, 1551 (1998); https://doi.org/10.1080/01496399808545055
275. J.Broome, S.Raymond. *Nature (London)*, **214**, 849 (1967); https://doi.org/10.1038/214849a0
276. E.R.Ramirez. *J. Am. Chem. Soc.*, **76**, 6237 (1954); https://doi.org/10.1021/ja01653a005
277. A.Klemm. *Angew. Chem.*, **70**, 21 (1958); https://doi.org/10.1002/ange.19580700105

278. K.Kontturi, P.Forssell, A.Ekman. *Sep. Sci. Technol.*, **17**, 1195 (1982); https://doi.org/10.1080/01496398208060644
279. A.Ekman, P.Forssell, K.Kontturi, G.Sundholm. *J. Membr. Sci.*, **11**, 65 (1982); https://doi.org/10.1016/S0376-7388(00)81243-0
280. P.Forssell, K.Kontturi. *Sep. Sci. Technol.*, **18**, 205 (1983); https://doi.org/10.1080/01496398308058331
281. K.Kontturi, T.Ojala, P.Forssell. *J. Chem. Soc. Faraday Trans. 1, Phys. Chem. Condens. Phases*, **80**, 3379 (1984); https://doi.org/10.1039/f19848003379
282. K.Kontturi, H.Pajari. *Sep. Sci. Technol.*, **21**, 1089 (1986); https://doi.org/10.1080/01496398608058399
283. K.Kontturi, A.-K.Kontturi, L.Pettersson, S.Karvinen, L.Niinistö, H.V.Volden, J.Weidlein, R.A.Zingaro. *Acta Chem. Scand.*, **40a**, 555 (1986); https://doi.org/10.3891/acta.chem.scand.40a-0555
284. K.Kontturi. *Sep. Sci. Technol.*, **21**, 591 (1986); https://doi.org/10.1080/01496398608056137
285. K.Kontturi. *Sep. Sci. Technol.*, **23**, 227 (1988); https://doi.org/10.1080/01496398808057644
286. L.M.Westerberg. *Sep. Sci. Technol.*, **23**, 235 (1988); https://doi.org/10.1180/claymin.1988.023.2.12
287. C.Tang, A.Yaroshchuk, M.L.Bruening. *Chem. Commun.*, **56**, 10954 (2020); https://doi.org/10.1039/D0CC03143G
288. C.Tang, M.P.Bondarenko, A.Yaroshchuk, M.L.Bruening. *J. Memb. Sci.*, **638**, 119684 (2021); https://doi.org/10.1016/j.memsci.2021.119684
289. C.Tang, A.Yaroshchuk, M.L.Bruening. *Membranes*, **12**, 631 (2022); https://doi.org/10.3390/membranes12060631
290. V.V.Sarapulova, E.L.Pasechnaya, V.D.Titorova, N.D.Pismenskaya, P.Y.Apel, V.V.Nikonenko. *Membr. Membr. Technol.*, **2**, 332 (2020); https://doi.org/10.1134/S2517751620050066
291. G.M.Geise, M.A.Hickner, B.E.Logan. *ACSAppl. Mater. Interfaces*, **5**, 10294 (2013); https://doi.org/10.1021/am403207w
292. Z.Ji, Q.Chen, J.Yuan, J.Liu, Y.Zhao, W.Feng. *Sep. Purif. Technol.*, **172**, 168 (2017); https://doi.org/10.1016/j.seppur.2016.08.006
293. S.Yang, Y.Liu, J.Liao, H.Liu, Y.Jiang, B.V.D.Bruggen, J.Shen, C.Gao. *ACSAppl. Mater. Interfaces*, **11**, 17730 (2019); https://doi.org/10.1021/acsami.8b21031
294. N.U.Afsar, X.Ge, Z.Zhao, A.Hussain, Y.He, L.Ge, T.Xu. *Sep. Purif. Technol.*, **254**, 117619 (2021); https://doi.org/10.1016/j.seppur.2020.117619
295. F.Sheng, L.Hou, X.Wang, M.Irfan, M.A.Shehzad, B.Wu, X.Ren, L.Ge, T.Xu. *J. Membr. Sci.*, **594**, 117453 (2020); https://doi.org/10.1016/j.memsci.2019.117453